Excitations in randomly diluted ferromagnets

Alba Theumann*
Laboratoire de Physique des Solides, Universite Paris-Sud, Centre d'Orsay, France

Raza A. Tahir-Kheli†
Department of Physics, Temple University, Philadelphia, Pennsylvania 19122
(Received 29 October 1974)

The dynamics of a randomly diluted quenched Heisenberg ferromagnet have recently been analyzed by several authors. Within an effective medium type of approach, the correct site aspect of this problem is best given by the recent work of Harris *et al.* Their theory, which introduces spurious degrees of freedom for the nonmagnetic vacancies and then projects them out by the use of an appropriate pseudopotential, however, works adequately for K vectors out to about halfway to the zone boundary and for low and intermediate concentrations of the nonmagnetic vacancies. For large vacancy concentrations, their results for the magnetic response leak over into the negative-frequency region. Also in their theory the spin-wave stiffness becomes complex for relative vacancy concentrations of order 49%. Here we present a new effective-medium approach to the study of this problem. We avoid the use of additional degrees of freedom for the vacancies by working directly with the equations of motion for the magnetic spins. Effective-medium ansatz is introduced through the use of a generalization of the path coherent-potential-approximation approach introduced by Brouers *et al.* in their study of random electronic alloys. For low and intermediate vacancy concentrations, our results are found to be of comparable quality to those given by Harris *et al.* However, unlike in their work, the first three frequency moments of the response are preserved exactly in our work. Moreover, on comparison with "exact" results—obtained via Padé procedures making use of numerically computed frequency moments—we find that our theory continues to yield qualitatively reasonable results even when the vacancy concentration is large, e.g., 60% in a simple-cubic lattice.

I. INTRODUCTION

In recent years much effort has been devoted to the task of describing the low-temperature dynamics of Heisenberg spin systems with substitutional disorder. The most rewarding theoretical framework for this purpose has been found to be the coherent-potential approximation (CPA). We present here yet another CPA approach to the problem. Because an adequate review of the current status of this field can be had by reading Harris *et al.*,[1] Theumann,[2] Tahir-Kheli,[3] Jones,[4] and others,[5-8] in the following we only give a description of the present work.

The purpose of this paper is to present a CPA[9] theory of the randomly diluted ferromagnet[1-8,10-12] which attempts to achieve two objectives: (i) A reformulation of the problem in such a way that the spurious degrees of freedom associated with nonmagnetic (empty) sites are not invoked at all and (ii) improvement in the quality of results for larger K vectors and for larger concentrations than that given by the Harris *et al.* CPA procedure.[1] In a matrix formulation of the equations of motion for the Green's functions in a simple-cubic lattice, we avoid the unphysical vacancy response by employing a random-phase-approximation (RPA)-like decoupling[13] of the magnetic spin Green's functions.

An important difference between the present work and the work of Harris *et al.*[1] is that by avoiding the boson representation, we sacrifice our ability to write the Hamiltonian for the dilute ferromagnet in terms of nonlocal perturbation potentials produced by vacancies. This implies that the effective medium cannot now be defined by means of nonlocal effective potentials at every site of the lattice. We have therefore to apply an alternative formulation of the CPA that is not based upon the multiple scattering theory for a perturbation potential, but instead is a generalization of the "path method" in the locator formalism.[14]

We describe briefly in Sec. II the general formulation of the problem and the effective medium. In Sec. III we discuss briefly the generalization of the path method and in Sec. IV we derive the self-consistent equations together with their solution in the dilute limit. Frequency moments of the response are discussed in Sec. V. Numerical results for the magnetic response, along with concluding remarks, are presented in Sec. VI.

II. FORMULATION: PRELIMINARY CONSIDERATIONS

We consider a simple-cubic lattice consisting of N lattice sites. On these sites we randomly distribute xN Heisenberg spins. Here x is the magnetic concentration, and $x \leq 1$. Making the assumption that the exchange interaction between any pair of magnetic atoms is independent of the presence, or the absence, of other magnetic atoms in the neighborhood, we can write the system Hamiltonian as

$$\mathcal{H}^c = -\sum_{i,j} c_i c_j J_{i,j} \vec{\sigma}_i \cdot \vec{\sigma}_j \ . \tag{2.1}$$

Here we introduce two simplifications. First, we assume the spatial range of the exchange interaction to be limited to the nearest-neighbor separation, i.e.,

$J_{i,j} = J_{j,i} = J$ if sites i and j are nearest neighbors,

$= 0$, otherwise.

Second, we restrict ourselves to considering the case where the spins are of magnitude $\frac{1}{2}$ (in Dirac's units). As will become clear in the following, the truncation of the range of $J_{i,j}$ simplifies our work nontrivially. On the other hand, the restriction to spin $\frac{1}{2}$ is not essential and the treatment is readily extended to the general spin case.

Variables c_i, c_j in Eq. (2.1) are the random-occupation variables such that $c_i = 1$ if the i site is occupied by a spin $\vec{\sigma}_i$, otherwise $c_i = 0$. We note that owing to the presence of these variables, the Hamiltonian in Eq. (2.1) is dependent upon the particular configuration specifying the distribution of xN magnetic spins upon the N sites. In thermal equilibrium, however, the properties of the system are determined entirely by the system temperature, the magnitude of the magnetic concentration x (we shall assume that the random distribution of the magnetic atoms has been "quenched" in), and the parameters of the Heisenberg exchange Hamiltonian, i.e., J, and the spin magnitude.

The original form of the coherent-potential approximation[9] was proposed to treat the effects of random local potentials in binary alloys. The problem becomes more complicated in the case of a disordered ferromagnet because the presence of an impurity, i.e., an empty site, in an otherwise uniform ferromagnet with nearest-neighbor interactions produces a nonlocal perturbation that extends to the first z neighbors of the impurity. It has therefore been recognized that the correct CPA approach to disordered magnets should take into account the exact form of the nonlocal perturbation.[10] The present approach consists in avoiding the use of the boson representation by working directly with the RPA equations of motion for the spin operators relevant to zero temperature, i.e.,

$$ic_i \frac{d\sigma_i^+}{dt} = \sum_n J_{i,n} c_i c_n (\sigma_i^+ - \sigma_n^+) \ . \tag{2.2}$$

Here we have explicitly invoked the fact that the magnitude of spin is $\frac{1}{2}$. Moreover, we have assumed a saturated ferromagnetic ground state. Thus,

$$2\sigma_n^z c_n \Omega_n \underset{T=0}{=} c_n \Omega_n \ , \tag{2.3}$$

whenever Ω_n is either a c number or it contains spin and occupation variables *not* referring to site n. Because Eq. (2.2), and any further equation of motion obtained therefrom, does not involve nonmagnetic sites, the spurious vacancy response is automatically suppressed without the introduction of a pseudopotential.

Second, because of the absence of an explicit perturbation potential in our formulation, we are led naturally to choosing an effective-medium formalism which, unlike the usual CPA theories, is not based upon multiple scattering theory.

To make these ideas precise, we commence our task by first defining a suitable effective medium. When this is done, we formally remove one of the effective-medium spins, placed upon site i say, and replace it by a "random" spin $c_i \vec{\sigma}_i$. This produces a perturbation which extends to the first-neighbor shell of the site i.

We define first the Hamiltonian of the frequency-dependent effective medium,

$$\mathcal{H}^{\text{eff}}(E) = -\sum_{i,j} \mathcal{J}_{i,j}^{\text{eff}}(E) \vec{S}_i \cdot \vec{S}_j \ . \tag{2.4}$$

As usual, the effective medium is isotropic and translationally uniform—i.e., all sites i are occupied by effective-medium spins S_i, and the exchange integral $\mathcal{J}_{i,j}^{\text{eff}}(E)$ depends only upon the separation $|R_i - R_j|$ and the complex frequency E. Because we assume the effects of a spin impurity to extend to the nearest-neighbor shell, it is therefore sufficient to restrict the spatial range of the effective-medium exchange integrals (which, of course, are in general complex) to a distance equal to twice the nearest-neighbor separation. Note that this is the largest separation between any two members of the seven-site cluster formed by the given central site and its six nearest neighbors. Moreover, because within such a cluster there are only three different types of intersite separations, we can make do by explicitly considering only three types of effective-medium exchange integrals, i.e.,

$$\mathcal{J}_{i,j}^{\text{eff}}(E) = \begin{cases} j_1(E) & \text{if } |R_i - R_j| = \delta_1 \\ j_2(E) & \text{if } |R_i - R_j| = \delta_2 \\ j_3(E) & \text{if } |R_i - R_j| = 2\delta_1 \ . \end{cases} \tag{2.5}$$

Here $\vec{\delta}_1$ and $\vec{\delta}_2$ are vectors connecting first- and second-neighbor sites, respectively.

It is convenient to study first the properties of the effective medium. Because we expect eventually to approximate the thermodynamic behavior of the random magnetic system by that of the uniform effective medium, we expect the equality of the magnetizations for the two systems, i.e.,

$$\langle S_i^z \rangle = \sum_{\{c\}} P(c) \langle c_i \sigma_i^z \rangle^c \equiv \langle c_i \sigma_i^z \rangle^T = \tfrac{1}{2} S^{\text{eff}}(T) \ . \tag{2.6}$$

Here the angular brackets, without the superscript c, signify a thermal average in the effective medium; we shall explicitly specify this averaging procedure later. $P(c)$ is the probability weight factor associated with configuration $\{c\}$ over which the configuration-dependent canonical average $\langle \cdots \rangle^c$ is taken. Summing such averages over all the configurations, as done on the right-hand side of Eq. (2.6), gives us the thermal average for the actual random system. Such an average is, here and henceforth, denoted by $\langle \cdots \rangle^T$.

Clearly, the right-hand side of Eq. (2.6) is equal to $\frac{1}{2}x$ at $T=0$, whenever the random magnetic system achieves a fully aligned ferromagnetic ground state. Hence the parameter $S^{\mathrm{eff}}(T=0)$ is equal to the magnetic concentration x.

To study the frequency–wave-vector-dependent response in the effective medium, i.e., $\rho_{\vec{K}}(\omega)$, we introduce the corresponding effective-medium Green's function, and note its RPA equation of motion:

$$g^{\mathrm{eff}}_{i,j}(E) = \Delta_0(E)\delta_{i,j} - \Delta_0(E)\sum_{\mu=1}^{3}\sum_{\delta_\mu} J_\mu(E)\, g^{\mathrm{eff}}_{i+\delta_\mu,j}(E)\,, \tag{2.7}$$

where $j_\mu(E)$ are as defined in Eq. (2.5) and

$$J_\mu(E) = S^{\mathrm{eff}}(T)\, j_\mu(E), \qquad \mu \equiv 1,2,3 \tag{2.8}$$

$$\Delta_0(E) = [E - 6J_1(E) - 12J_2(E) - 6J_3(E)]^{-1}. \tag{2.9}$$

[Note that $J_\mu(E)$, etc., are related to the energy-dependent, effective-medium exchange and are not to be confused with the actual exchange integrals $J_{i,j}$, etc.] Because the effective medium is translationally invariant, it is convenient to Fourier transform Eq. (2.7) to inverse lattice space, i.e.,

$$g^{\mathrm{eff}}_{\vec{K}}(E) = [\Delta_0^{-1}(E) + 6J_1(E)\gamma_{\vec{K}} + 12J_2(E)\nu_{\vec{K}} + 6J_3(E)\gamma_{2\vec{K}}]^{-1}, \tag{2.10}$$

where, measuring the unit of length in terms of the cube edge,

$$g^{\mathrm{eff}}_{i,j}(E) = \frac{1}{N}\sum_{\vec{K}} g^{\mathrm{eff}}_{\vec{K}}(E)\, e^{i\vec{K}\cdot(\vec{i}-\vec{j})}\,, \tag{2.11}$$

$$\gamma_{\vec{K}} = \sum_{\vec{\delta}_1} \tfrac{1}{6} e^{i\vec{K}\cdot\vec{\delta}_1} = \tfrac{1}{3}[\cos K_x + \cos K_y + \cos K_z]\,,$$

$$\nu_{\vec{K}} = \sum_{\vec{\delta}_2} \tfrac{1}{12} e^{i\vec{K}\cdot\vec{\delta}_2} = \tfrac{1}{4}[6(\gamma_{\vec{K}})^2 - 1 - \gamma_{2\vec{K}}]\,. \tag{2.12}$$

Having thus defined the effective medium, we turn to the description of a path method,[14] which will enable us to derive the conditions necessary for the identification of the effective-medium properties with those of the actual random system (when the later is in thermodynamic equilibrium).

To facilitate algebraic manipulations and to help specify the appropriate path-method ansatz for the problem in hand, in the following we will indicate by a Greek subindex, $\alpha, \beta, \ldots$, the positions of the first neighbors of the site i, while a subindex s will indicate any atom in the cluster, i.e., s denotes either α or i.

We remind ourselves here that so far we have achieved a description of the uniform effective medium. Moreover, we also know the exchange parameters of the actual (random) system. Yet, if we are to proceed with the analysis related to the imbedding of an actual spin, or an actual vacancy, on an arbitrary site within the medium, we have to specify what the exchange interactions between the random spin and the medium are. Indeed, we have to further address ourselves to the question of how the exchange interactions between any pair of the six members of the first-neighbor shell (of site i) are modified by the presence of a random spin on the central site.

Unfortunately, the existing work on the path CPA method[14] does not offer any guidance in this matter. The reason for this is clear. Whereas in the literature the path method has previously been applied only to the case of alloys with diagonal, on-site, random interactions—for which it is not necessary to specify the interaction between the effective medium and the actual (random) atom—in the present study both the diagonal and the off-diagonal interactions are random. Moreover, here the diagonal part of the interaction is also dependent upon the environment of the atom in question—a situation which is not envisioned in the usual works on alloys.

Therefore, it is necessary to make an appropriate specification of these interactions:

(a) Regarding the interaction between the random spin $c_i\vec{\sigma}_i$ and its first-neighbor shell of coherent (effective medium) spins S_α, we argue as follows: If any of the coherent spins S_α were also replaced by another random spin, then the exchange interaction between the two spins would, of course, be equal to J. Similarly when the site i also has a coherent spin S_i rather than a random one, the corresponding exchange between it and its neighbor is $j_1(E)$. Hence, it is reasonable to assume that the interaction that obtains between a random spin $c_i\vec{\sigma}_i$ and its neighboring effective-medium spin S_α is equal to $j_1'(E)$, which is given by the average of the two situations, i.e.,

$$j_1'(E) = \tfrac{1}{2}[J + j_1(E)]\,. \tag{2.13a}$$

(b) Next we consider the interaction between the central site i and members of the effective medium outside the first-neighbor shell. As is generally accepted, the philosophy of CPA-like[9] and path-type[14] methods is to assume a limited spatial range of perturbation caused by the removal of an effective-medium atom and its subsequent replacement by an actual random atom. In line with this phi-

losophy, here we assume the range of perturbation *not to extend beyond the nearest-neighbor distance from the central site.* Of course, in a more detailed and careful treatment, one may want to extend the spatial range of such a perturbation, but within the present approximation scheme, where we embed only one random spin, rather than several in a compact cluster, this does not seem warranted. Therefore, we conclude that a reasonable choice for interactions between the random spin and members of the medium outside the neighboring shell is to assume that they are the same as they would have been if no random spin had been substituted at the central location i.

(c) Next let us consider the choice of interactions between any two members of the six spins in the first-neighbor shell. Clearly, there are two different types of configurations for any such pair. First, there are pairs of sites which are noncollinear with the central site, e.g., sites (1, 0, 0) and (0, 1, 0), if the central site is denoted as (0, 0, 0). Second, there are collinear pairs, e.g., (1, 0, 0) and (−1, 0, 0).

Before we proceed further with the examination of what an appropriate choice of the interaction between the former and the latter type of pairs of sites should be, we hasten to emphasize that even though both these types of pairs are separated by distances larger than the neighboring separation, 1, they both involve the presence of the perturbing random site at the center of the shell. Hence, both sites of each of these pairs are *within reach* of the assumed range of the perturbation placed at the central site.

A useful way of looking at the occurrence of $j_2(E)$ and $j_3(E)$, i.e., the larger-range exchange integrals within the effective medium, is as follows: In the absence of the perturbing random spin at (0, 0, 0), $j_2(E)$ between, say, the pair (1, 0, 0) and (0, 1, 0) may be thought to be communicated via the two possible paths (1, 0, 0) → (0, 0, 0) → (0, 1, 0) and (1, 0, 0) → (1, 1, 0) → (0, 1, 0). (Note, all other paths are longer than these two.) Now, when a perturbing potential is interposed at (0, 0, 0), *cutting* the former of the two paths, it is reasonable to assume that as a result the interaction between (1, 0, 0) and (0, 1, 0) is reduced to half its usual strength within the medium; i.e., it becomes $j_2'(E)$ such that

$$j_2'(E)=\tfrac{1}{2}j_2(E)\ . \tag{2.13b}$$

Finally, let us examine the interaction between sites of the type α and $-\alpha$, e.g., between (1, 0, 0) and (−1, 0, 0). Here, the relevant shortest path is unique and it goes via the central site (0, 0, 0). Thus when the medium spin is abstracted from this location—and a perturbing random spin substituted, instead—it is reasonable to assume that the corresponding interaction is cut off altogether, i.e., that it becomes $j_3(E)$ such that

$$j_3'(E)=0\ . \tag{2.13c}$$

In the above, we have dwelt in some detail on the choice of $j_\mu'(E)$. We feel this to be fully justified, since no *a priori* guidance in this matter is available in the existing literature. Because the various Green's functions referring to the cluster (centered at i) involve one or more effective-medium spins, therefore they can be obtained quite simply from the following two RPA "time derivatives":

$$i\frac{d(c_i\sigma_i^+)}{dt}=\sum_\alpha \tfrac{1}{2}[J+j_1(E)](2\langle S_\alpha^z\rangle c_i\sigma_i^+ - 2c_i\langle\sigma_i^z\rangle^T S_\alpha^+) + \sum_{n\neq s} j_{i,n}^{\rm eff}(E)(2\langle S_n^z\rangle c_i\sigma_i^+ - 2c_i\langle\sigma_i^z\rangle^T S_n^+), \tag{2.14a}$$

$$i\frac{dS_\alpha^+}{dt}=\tfrac{1}{2}[J+j_1(E)](2c_i\langle\sigma_i^z\rangle^T S_\alpha^+ - 2\langle S_\alpha^z\rangle c_i\sigma_i^+) + \sum_{\beta\neq-\alpha}\tfrac{1}{2}j_2(E)(2\langle S_\beta^z\rangle S_\alpha^+ - 2\langle S_\alpha^z\rangle S_\beta^+) + \sum_{n\neq s} j_{\alpha,n}^{\rm eff}(E)(2\langle S_n^z\rangle S_\alpha^+ - 2\langle S_\alpha^z\rangle S_n^+). \tag{2.14b}$$

[Note that these equations make use of the ansatz (2.13a)–(2.13c).] The last terms in Eqs. (2.14a) and (2.14b) are sums over sites outside the nearest-neighbor cluster. (Recall that the subscript s refers to any of the seven sites of the cluster, and α, β, etc., to any of the six sites in the first-neighbor shell of site i.)

In what follows we shall assume the system temperature to be zero. Hence we shall write

$$2\langle S_\alpha^z\rangle = S^{\rm eff}(T=0)\equiv S^{\rm eff}\ ,\qquad 2c_i\langle\sigma_i^z\rangle^T \underset{T=0}{=} c_i\ . \tag{2.14c}$$

From Eqs. (2.14a)–(2.14c) we obtain the following compact expression for the RPA equations of motion for the energy Fourier transform of the composite Green's function in the cluster:

$$g_{i,s}(E)=g_i^0(E)\delta_{i,s}-g_i^0(E)\sum_\alpha J_1'(E)g_{\alpha,s}(E)-g_i^0(E)\sum_{n\neq s}J_{i,n}^{\rm eff}(E)g_{n,s}(E)\ , \tag{2.15}$$

$$g_{\alpha,s}(E)=g_\alpha^0(E)\delta_{\alpha,s}-g_\alpha^0(E)\left(J_1'(E)g_{i,s}(E)+\sum_{\beta\neq-\alpha}J_2'(E)g_{\beta,s}(E)\right)-g_\alpha^0(E)\sum_{n\neq s}J_{\alpha,n}^{\rm eff}(E)g_{n,s}(E)\ . \tag{2.16}$$

Here the subscript s denotes either the central atom i or one of the six atoms α in the shell. Also, as defined in Eqs. (2.5), (2.8), and (2.14c), we have

$$J^{\rm eff}_{s,n}(E) = S^{\rm eff} j^{\rm eff}_{s,n}(E) \ . \tag{2.17a}$$

The notation for primed exchange integrals is similar, i.e.,

$$J'_1(E) = S^{\rm eff} j'_1(E) = \tfrac{1}{2}[S^{\rm eff} J + J_1(E)] \ , \tag{2.17b}$$

$$J'_2(E) = S^{\rm eff} j'_2(E) = \tfrac{1}{2} S^{\rm eff} j_2(E) = \tfrac{1}{2} J_2(E) \ . \tag{2.17c}$$

[Compare Eqs. (2.13a) and (2.13b).] The remaining notation, in Eqs. (2.15) and (2.16), referring to the central and shell-site locators, is as follows:

$$g^0_i(E) = (c_i/S^{\rm eff})\{\Delta_0^{-1}(E) + 3[J_1(E) - S^{\rm eff} J]\}^{-1} \ , \tag{2.18}$$

$$g^0_\alpha(E) = [\Delta_0^{-1}(E) + \epsilon_1(E)]^{-1} \ , \tag{2.19}$$

where $\Delta_0(E)$ is as defined in Eq. (2.9) and

$$\epsilon_1(E) = J_1(E) - (c_i/2S^{\rm eff})[S^{\rm eff} J + J_1(E)] + 2J_2(E) + J_3(E) \ . \tag{2.20}$$

We observe from Eqs. (2.19) and (2.20) that even though the shell sites α are occupied by the medium spins S_α, owing to the nonlocal character of the exchange interactions, the shell locator $g^0_\alpha(E)$ is modified by the presence of a random spin $c_i\sigma_i$ at the center.

III. FORMULATION: GENERALIZED-PATH METHOD

We now begin the formulation of a generalized-path CPA procedure, referred to in the preceding sections. The present format of this procedure is necessarily different from that used by Brouers *et al.* and by Brouers and Ducastelle[14] for two basic reasons. First, unlike in these works, we need to consider here both the off-diagonal randomness as well as the nonlocal character of the diagonal randomness. Second, even if differences in the characters of the potentials for the two problems were not present, our present formulation would still be in the nature of a generalization of the works referred to in Ref. 14, because in our work we take a proper account of the crystal symmetry of the lattice, whereas Brouers *et al.*[14] dealt with it in an approximate fashion, and also we do not introduce any decoupling approximation for the occupation variables of the clusters.

We start by combining Eqs. (2.15) and (2.16) in a compact expression:

$$g_{s,s'}(E) = g^0_s(E)\delta_{s,s'} - g^0_s(E) \sum_{s''} J'_{s,s''}(E) g_{s'',s'}(E) - g^0_s(E) \sum_n J^{\rm eff}_{s,n}(E) g_{n,s'}(E) \ . \tag{3.1}$$

Note that s refers to any atom in the seven-atom cluster and $J'_{s,s'}(E)$ takes the values

$$J'_{s,s'}(E) = \begin{cases} J'_1(E) & \text{if } s = i \text{ and } s' = \alpha, \text{ or vice versa} \\ J'_2(E) & \text{if } s = \alpha \text{ and } s' = \beta \neq -\alpha, \text{ or vice versa} \\ J'_3(E) = 0 & \text{if } s = \alpha \text{ and } s' = -\alpha, \text{ or vice versa} \end{cases} \tag{3.2}$$

and moreover $J^{\rm eff}_{s,n}(E)$ and $J'_\mu(E)$ are as defined in Eqs. (2.17a)–(2.17c).

The last term in Eq. (3.1) connects an atom s in the shell with the effective medium outside the shell. Therefore, it is clear that a diagrammatic expansion of $g_{s,s'}(E)$ will sum the terms shown in Fig. 1(a), which in turn can be resummed to give the integral equation shown in Fig. 1(b), i.e.,

$$g_{s,s'}(E) = g^0_s(E)\delta_{s,s'} - g^0_s(E) \sum_{s''} [J'_{s,s''}(E) + H_{s,s''}(E)] g_{s'',s'}(E) \ . \tag{3.3}$$

In this equation, we note that the only sites which are explicitly mentioned lie *within* the seven-site cluster. This is quite a remarkable situation because all our previous relationships have involved references to sites outside the cluster. Because this situation has been brought about through the introduction of $H_{s,s''}(E)$, let us, therefore, look a little more carefully at this quantity.

The quantity $H_{s,s''}(E)$ is shown in Fig. 1(c) and sums all the paths that leave site s, go outside the shell, and come back to the site s''. The functions $H_{s,s''}(E)$ are completely determined by the effective medium, which is isotropic and also translationally invariant; hence they depend only on the relative distance $|R_s - R_{s''}|$. Taking into account the symmetry of the simple-cubic lattice we have only five different values for $H_{s,s'}(E)$:

$$H_{s,s'}(E) = \begin{cases} H_{00}(E) & \text{if } s = s' = i \\ H_0(E) & \text{if } s = s' = \alpha \\ H_1(E) & \text{if } s\ (s') = i \text{ and } s'\ (s) = \alpha \\ H_2(E) & \text{if } s\ (s') = \alpha \text{ and } s'\ (s) = \beta \neq -\alpha \\ H_3(E) & \text{if } s\ (s') = \alpha \text{ and } s'\ (s) = -\alpha \ . \end{cases} \tag{3.4}$$

Equation (3.3) is similar to the set of equations derived by Brouers *et al.* and Brouers and Ducastelle,[14] except that in their case only $H_0(E)$, $H_2(E)$, and $H_3(E)$ appear, as they consider only nearest-neighbor hopping. Also they approximate $H_{s,s'}(E)$ by an average form that does not reproduce the complete crystal symmetry. We avoid this approximation by writing Eq. (3.3) in a compact matrix form and by using the crystal symmetry group to simplify the equations.

We introduce 7×7 matrices, whose rows and columns are labeled by the central site i and its six neighbors distributed in pairs of opposite sites. We can then write Eq. (3.3):

$$\bar{g}=[\bar{1}+\bar{g}^0\bar{H}]^{-1}\bar{g}^0\,, \tag{3.5}$$

where

$$\bar{g}=\begin{vmatrix} g_{i,i}(E) & g_{i,1}(E) & g_{i,-1}(E) & g_{i,2}(E) & g_{i,-2}(E) & g_{i,3}(E) & g_{i,-3}(E) \\ g_{1,i}(E) & \cdot & \cdot & \cdot & \cdot & \cdot & \cdot \\ g_{-1,i}(E) & \cdot & \cdot & \cdot & \cdot & \cdot & \cdot \\ g_{2,i}(E) & \cdot & \cdot & \cdot & \cdot & \cdot & \cdot \\ g_{-2,i}(E) & \cdot & \cdot & \cdot & \cdot & \cdot & \cdot \\ g_{3,i}(E) & \cdot & \cdot & \cdot & \cdot & \cdot & \cdot \\ g_{-3,i}(E) & \cdot & \cdot & \cdot & \cdot & \cdot & \cdot \end{vmatrix}, \tag{3.6}$$

(we denote by dots the remaining matrix elements; they can be easily identified by inspection),

$$\bar{g}^0=\begin{vmatrix} g_i^0(E) & 0 & 0 & 0 & 0 & 0 & 0 \\ 0 & g_1^0(E) & 0 & 0 & 0 & 0 & 0 \\ 0 & 0 & g_{-1}^0(E) & 0 & 0 & 0 & 0 \\ 0 & 0 & 0 & g_2^0(E) & 0 & 0 & 0 \\ 0 & 0 & 0 & 0 & g_{-2}^0(E) & 0 & 0 \\ 0 & 0 & 0 & 0 & 0 & g_3^0(E) & 0 \\ 0 & 0 & 0 & 0 & 0 & 0 & g_{-3}^0(E) \end{vmatrix}, \tag{3.7}$$

$$\bar{K}=\begin{vmatrix} H_{00}(E) & \downarrow & \downarrow & \downarrow & \downarrow & \downarrow & \downarrow \\ \downarrow & H_0(E) & H_3(E) & \rightarrow & \rightarrow & \rightarrow & \rightarrow \\ \downarrow & H_3(E) & H_0(E) & \rightarrow & \rightarrow & \rightarrow & \rightarrow \\ \downarrow & \rightarrow & \rightarrow & H_0(E) & H_3(E) & \rightarrow & \rightarrow \\ \downarrow & \rightarrow & \rightarrow & H_3(E) & H_0(E) & \rightarrow & \rightarrow \\ \downarrow & \rightarrow & \rightarrow & \rightarrow & \rightarrow & H_0(E) & H_3(E) \\ \downarrow & \rightarrow & \rightarrow & \rightarrow & \rightarrow & H_3(E) & H_0(E) \end{vmatrix}. \tag{3.8}$$

Here a horizontal arrow indicates that the relevant matrix element is equal to $H_2(E)+J_2'(E)$. On the other hand, a vertical arrow denotes that the indicated location has a matrix element equal to $H_1(E)+J_1(E)$. Finally, $g_i^0(E)$ and $g_\alpha^0(E)$ are as given in Eqs. (2.18) and (2.19).

We note that all the matrices on the right-hand side of Eq. (3.5) have the general form

$$\bar{M}=\begin{vmatrix} m_{00} & m_1 & m_1 & m_1 & m_1 & m_1 & m_1 \\ m_1 & m_0 & m_3 & m_2 & m_2 & m_2 & m_2 \\ m_1 & m_3 & m_0 & m_2 & m_2 & m_2 & m_2 \\ m_1 & m_2 & m_2 & m_0 & m_3 & m_2 & m_2 \\ m_1 & m_2 & m_2 & m_3 & m_0 & m_2 & m_2 \\ m_1 & m_2 & m_2 & m_2 & m_2 & m_0 & m_3 \\ m_1 & m_2 & m_2 & m_2 & m_2 & m_3 & m_0 \end{vmatrix}. \tag{3.9}$$

therefore they can all be block diagonalized by means of a unitary transformation $\bar{U}$ as described by Wolfram and Callaway.[7] By introducing the matrix

$$\bar{U}=\begin{vmatrix} 1 & 0 & 0 & 0 & 0 & 0 & 0 \\ 0 & a & b & 0 & 0 & 0 & 2d \\ 0 & a & -b & 0 & 0 & 0 & 2d \\ 0 & a & 0 & b & 0 & c & -d \\ 0 & a & 0 & -b & 0 & c & -d \\ 0 & a & 0 & 0 & b & -c & -d \\ 0 & a & 0 & 0 & -b & -c & -d \end{vmatrix}, \tag{3.10}$$

with $a^{-1}=\sqrt{6}$, $b^{-1}=\sqrt{2}$, $c=\frac{1}{2}$, $d^{-1}=\sqrt{12}$, we obtain from Eqs. (3.9) and (3.10):

$$\bar{M}_T \equiv \bar{U}^{\dagger}\bar{M}\bar{U}=\begin{vmatrix} \bar{M}_s & 0 & 0 & 0 & 0 & 0 \\ 0 & m_p & 0 & 0 & 0 & 0 \\ 0 & 0 & m_p & 0 & 0 & 0 \\ 0 & 0 & 0 & m_p & 0 & 0 \\ 0 & 0 & 0 & 0 & m_d & 0 \\ 0 & 0 & 0 & 0 & 0 & m_d \end{vmatrix}, \tag{3.11}$$

where $\bar{M}_s$ is a 2×2 matrix,

$$\bar{M}_s=\begin{vmatrix} m_{00} & \sqrt{6}\,m_1 \\ \sqrt{6}\,m_1 & m_s \end{vmatrix}, \tag{3.12}$$

and

$$\begin{aligned} m_s &= m_0+m_3+4m_2\,, \\ m_p &= m_0-m_3\,, \\ m_d &= m_0+m_3-2m_2\,. \end{aligned} \tag{3.13}$$

We shall use this notation throughout the remainder of this paper. Moreover, because under the unitary transformation $\bar{U}$ all the matrices reflecting simple-cubic crystal symmetry transform to give the same type of structure as given in Eq. (3.11), therefore we shall henceforth use the corresponding notation without making any explicit mention thereof. Transforming the Green's-function matrix given in Eq. (3.5) under the unitary transformation (3.10), after some algebraic manipulations we are led to the following results for the various components of $\bar{g}_T$:

$$\bar{g}_s=[(\bar{h})^{-1}+\bar{P}\cdot\bar{H}_s]^{-1}\bar{P}\,, \tag{3.14}$$

$$g_\eta=[\Delta_0^{-1}(E)+\epsilon_1(E)+H_\eta(E)]^{-1}\,, \quad \eta\equiv p,d \tag{3.15}$$

where $\epsilon_1(E)$ is as given in Eq. (2.20),

$$(\bar{h})^{-1}=\begin{vmatrix} S^{\mathrm{eff}}[\Delta_0^{-1}(E)+3(J_1(E)-S^{\mathrm{eff}}J)] & 0 \\ 0 & \Delta_0^{-1}(E)+\epsilon_1(E) \end{vmatrix} \tag{3.16}$$

and

$$\bar{P}=\begin{vmatrix} c_i & 0 \\ 0 & 1 \end{vmatrix}. \tag{3.17}$$

[Note, that while transforming $\bar{g}^0$, we made use of the relations (2.18) and (2.19) which defined the various components, i.e., $g_i^0(E)$ and $g_\alpha^0(E)$, of this matrix.]

We can see from Eq. (3.17) that because $(c_i)^2=c_i$, therefore $(\bar{P})^2=\bar{P}$. Hence the matrix $\bar{P}$ is a projection operator over the two states of occupation of the site i. We emphasize that it is the pres-

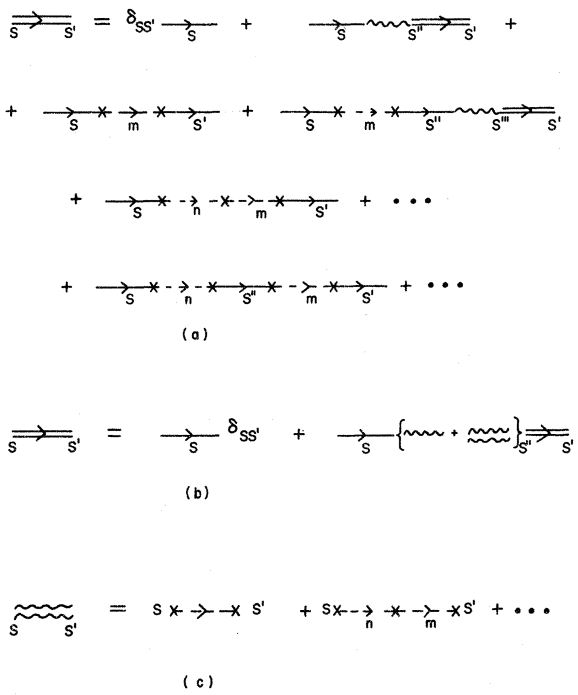

FIG. 1. (a) Diagrammatic expansion of $g_{s,s'}(E)$, according to Eq. (3.1) in the test. (b) Integral equation for $g_{s,s'}(E)$. (c) Diagrams which contribute to $H_{s,s'}(E)$. In (a)–(c), a single continuous line with an arrow represents the bare locator referring to one of the atoms of the cluster. Double lines with an arrow denote the Green's function $g_{s,s'}(E)$, and a broken line with an arrow represents the effective-medium locator $\Delta_0(E)$. A single wiggly line stands for the in-shell interaction of the form $J'_{s,s'}(E)$, while a double wiggly line represents the factor $H_{s,s'}(E)$. Finally, the effective interactions of the form $J^{\mathrm{eff}}_{l,j}(E)$ are represented by crosses subject to the condition that either l or j may be a member of the cluster but l and j are not simultaneously members of the cluster. Note that as in the text, sites labeled by s are members of the cluster while n, m, ... indicate sites in the medium.

ence of $\bar{P}$ in an RPA description of the equations of motion, in contrast to the spin-wave formalism, which makes unnecessary the introduction of a pseudopotential in the formulation.

The components of the matrix $\bar{H}_T$ are similarly obtained from Eqs. (3.8), (3.12), and (3.13), and we get

$$\bar{H}_s = \begin{vmatrix} H_{00}(E) & \sqrt{6}[J_1'(E)+H_1(E)] \\ \sqrt{6}[J_1'(E)+H_1(E)] & H_s(E) \end{vmatrix} \tag{3.18}$$

and

$$\begin{aligned} H_s(E) &= H_0(E)+H_3(E)+4[H_2(E)+J_2'(E)] \ , \\ H_p(E) &= H_0(E)-H_3(E) \ , \\ H_d(E) &= H_0(E)+H_3(E)-2[H_2(E)+J_2'(E)] \ . \end{aligned} \tag{3.19}$$

[Confusion between the matrix $\bar{H}_s$ and one of its components $H_s(E)$ should not arise.]

Our next task is to express the components of $\bar{H}_T$ in terms of the effective-medium Green's functions. Using Eq. (2.7), the relevant equations of motion for $g^{\mathrm{eff}}_{s,s'}(E)$, referring to sites *within* the cluster, are readily obtained:

$$g^{\mathrm{eff}}_{s,s'}(E) = \Delta_0(E)\left(\delta_{s,s'} - \sum_{s''} J^{\mathrm{eff}}_{s,s''}(E) g^{\mathrm{eff}}_{s'',s'}(E) - \sum_{n}{}' J^{\mathrm{eff}}_{s,n}(E) g^{\mathrm{eff}}_{n,s'}(E)\right) \ . \tag{3.20}$$

The primed sum $\sum_n'$, occurring in the last term on the right-hand side of Eq. (3.20), indicates a sum over sites n which are outside the seven sites of the cluster. [To avoid notational confusion, it should be mentioned that the spin referring to the central site i in Eq. (3.1) was an actual random spin, whereas in Eq. (3.20) the entire cluster consists of the effective-medium spins.]

Observing the structure of Eq. (3.20) we readily conclude that it is similar to that of Eq. (3.1), which referred to the composite Green's functions. The only differences are that in (3.20) we have the effective-medium locator $\Delta_0(E)$ and the effective exchange $J^{\mathrm{eff}}_{s,s'}(E)$, whereas in Eq. (3.1), correspondingly we have the cluster atomic locators $g^0_s(E)$ and the primed exchange interactions $J'_{s,s'}(E)$. Hence, in complete analogy with the derivation of Eq. (3.3), we get

$$g^{\mathrm{eff}}_{s,s'}(E) = \Delta_0(E)\delta_{s,s'} - \Delta_0(E)\sum_{s''}[J^{\mathrm{eff}}_{s,s''}(E) + H_{s,s''}(E)] g^{\mathrm{eff}}_{s'',s'}(E) \ . \tag{3.21}$$

The important point to note here is that the same set of parameters $H_{s,s'}(E)$ occur in Eqs. (3.3) and (3.21). [See Fig. 1(c) for a diagrammatic representation of these quantities.]

Let us introduce the matrix notation $\bar{g}^{\mathrm{eff}}$ for the set of 49 matrix elements $g^{\mathrm{eff}}_{s,s'}(E)$ arranged and labeled in an analogous manner to the matrix elements of $\bar{g}$, given on the right-hand side of Eq. (3.6). Then the corresponding block-diagonalized matrix $\bar{g}^{\mathrm{eff}}_T$ is readily found. The relevant elements are

$$\bar{g}^{\mathrm{eff}}_s = [\Delta_0^{-1}(E)\bar{1} + \bar{H}^{\mathrm{eff}}_s]^{-1} \ , \tag{3.22}$$

$$g^{\mathrm{eff}}_\eta = [\Delta_0^{-1}(E) + H^{\mathrm{eff}}_\eta(E)]^{-1} \ , \quad \eta \equiv p, d \tag{3.23}$$

where

$$\bar{H}^{\mathrm{eff}}_s = \begin{vmatrix} H_{00}(E) & \sqrt{6}[J_1(E)+H_1(E)] \\ \sqrt{6}[J_1(E)+H_1(E)] & H^{\mathrm{eff}}_s(E) \end{vmatrix} , \tag{3.24}$$

$$\begin{aligned} H^{\mathrm{eff}}_s(E) &= H_0(E)+H_3(E)+J_3(E)+4[H_2(E)+J_2(E)] \ , \\ H^{\mathrm{eff}}_p(E) &= H_0(E)-H_3(E)-J_3(E) \ , \\ H^{\mathrm{eff}}_d(E) &= H_0(E)+H_3(E)+J_3(E)-2H_2(E)-2J_2(E) \ . \end{aligned} \tag{3.25}$$

By comparing Eqs. (3.24) and (3.25) with Eqs. (3.18) and (3.19), and taking into account the definition of $J_1'(E)$ and $J_2'(E)$ given in Eqs. (2.17b) and (2.17c), we can write

$$\bar{H}_s = \bar{H}^{\mathrm{eff}}_s - \bar{\Delta}_s = (\bar{g}^{\mathrm{eff}}_s)^{-1} - \Delta_0^{-1}(E)\bar{1} - \bar{\Delta}_s \ , \tag{3.26}$$

$$H_p(E) = H^{\mathrm{eff}}_p(E) + J_3(E) = (g^{\mathrm{eff}}_p)^{-1} - \Delta_0^{-1}(E) + J_3(E) \ , \tag{3.27}$$

$$H_d(E) = H^{\mathrm{eff}}_d(E) + J_2(E) - J_3(E) = (g^{\mathrm{eff}}_d)^{-1} - \Delta_0^{-1}(E) + J_2(E) - J_3(E) \ , \tag{3.28}$$

where

$$\bar{\Delta}_s = \begin{vmatrix} 0 & \frac{1}{2}\sqrt{6}[J_1(E) - S^{\mathrm{eff}}J] \\ \frac{1}{2}\sqrt{6}[J_1(E) - S^{\mathrm{eff}}J] & 2J_2(E)+J_3(E) \end{vmatrix} . \tag{3.29}$$

By introducing Eqs. (3.26)–(3.29) into Eqs. (3.14) and (3.15), we get

$$\bar{g}_s = [\bar{V}_s + \bar{P}(\bar{g}^{\mathrm{eff}}_s)^{-1}]\bar{P} \tag{3.30}$$

and

$$g_\eta = [V_\eta + (g^{\mathrm{eff}}_\eta)^{-1}]^{-1} \ , \quad \eta \equiv p, d \ . \tag{3.31}$$

In the above we have used the notation

$$\bar{V}_s = (\bar{h})^{-1} - \bar{P}[\Delta_0^{-1}(E)\bar{1} + \bar{\Delta}_s] \ . \tag{3.32}$$

From Eqs. (3.16), (3.17), and (3.29) a more explicit expression for $\bar{V}_s$ can be obtained, i.e.,

$$\bar{V}_s = \begin{vmatrix} (S^{\text{eff}} - c_i)\,\Delta_0^{-1}(E) + 3S^{\text{eff}}[J_1(E) - S^{\text{eff}}J] & -\tfrac{1}{2}\sqrt{6}\,c_i[J_1(E) - S^{\text{eff}}J] \\ -\tfrac{1}{2}\sqrt{6}[J_1(E) - S^{\text{eff}}J] & \epsilon_1(E) - 2J_2(E) - J_3(E) \end{vmatrix} , \tag{3.33}$$

where $\epsilon_1(E)$ is the same as in Eq. (2.20). Explicit expressions for V_η are found more readily, i.e., we get

$$V_p = J_1(E) - (c_i/2S^{\text{eff}})[J_1(E) + S^{\text{eff}}J] + 2J_2(E) + 2J_3(E) , \tag{3.34}$$

$$V_d = J_1(E) - (c_i/2S^{\text{eff}})[J_1(E) + S^{\text{eff}}J] + 3J_2(E) . \tag{3.35}$$

The foregoing equations, i.e., Eqs. (3.29)–(3.35), can now be used to write down explicit expressions for the configuration-dependent Green's functions for the cluster.

Because we are using the irreducible representation, all these Green's functions are specified by the 2×2 matrix $\bar{g}_s$ and the p and d components, g_η.

It is clear that in order to derive self-consistent relations for the basic unknowns of our theory, i.e., $J_\mu(E)$, we have to carry out a configurational average—of these configuration-dependent Green's functions—over the two modes of occupancy of the central site i. This task is undertaken in Sec. IV.

IV. SELF-CONSISTENT EQUATIONS

The concept of configurational averaging was defined explicitly in Sec. II [see the right-hand side of Eq. (2.6)]. Because, the set of equations (3.30)–(3.35) depend upon the occupancy of only the central site i, we can perform the configurational averaging by computing the values of the quantity being averaged for two cases, $c_i = 1$ and $c_i = 0$, separately and then by weighting those values according to the probability factors x and $1-x$, respectively. In this manner, using Eqs. (3.23), (3.31), (3.34), and (3.35), we get for $T = 0$, where $S^{\text{eff}} = x$,

$$\langle g_\eta \rangle^{T=0} = x\{Z_\eta(E) - (1/2x)[Jx + J_1(E)] + (g_\eta^{\text{eff}})^{-1}\}^{-1} + (1-x)[Z_\eta(E) + (g_\eta^{\text{eff}})^{-1}]^{-1} , \quad \eta \equiv p, d . \tag{4.1}$$

For simplicity here we have introduced the notation

$$Z_p(E) = J_1(E) + 2[J_2(E) + J_3(E)] , \qquad Z_d(E) = J_1(E) + 3J_2(E) . \tag{4.2}$$

In effect, therefore, the three self-consistent parameters of our theory may be considered to be $J_1(E)$, $Z_p(E)$, and $Z_d(E)$.

Next, we deal with the 2×2 matrix quantity $\bar{g}_s$ given in (3.30). Its configurational average is similarly straightforward to obtain and we get

$$\langle \bar{g}_s \rangle^{T=0} = x[\bar{V}_1 + (\bar{g}_s^{\text{eff}})^{-1}]^{-1}\bar{P}_1 + (1-x)[\bar{V}_0 + \bar{P}_0(g_s^{\text{eff}})^{-1}]^{-1}\bar{P}_0 . \tag{4.3}$$

Note that the projection operator $\bar{P}$ defined in Eq. (3.17) is a unit matrix for the case of magnetic occupancy of the central site, i.e.,

$$(\bar{P})_{c_i=1} \equiv \bar{P}_1 = \bar{1} . \tag{4.4}$$

Similarly, when $c_i = 0$,

$$(\bar{P})_{c_i=0} \equiv \bar{P}_0 = \begin{vmatrix} 0 & 0 \\ 0 & 1 \end{vmatrix} . \tag{4.5}$$

Regarding the matrices $\bar{V}_0$ and $\bar{V}_1$ in Eq. (4.3), these are readily seen to be

$$\bar{V}_0 = (\bar{V}_s)_{c_i=0} = \begin{vmatrix} x\Delta_0^{-1}(E) + 3x[J_1(E) - xJ] & 0 \\ -\tfrac{1}{2}\sqrt{6}[J_1(E) - xJ] & J_1(E) \end{vmatrix} , \tag{4.6}$$

$$\bar{V}_1 = (\bar{V}_s)_{c_i=1} = \begin{vmatrix} B_{00} & \sqrt{6}B_1 \\ \sqrt{6}B_1 & B_s \end{vmatrix} , \tag{4.7a}$$

where

$$B_{00} = -(1-x)\Delta_0^{-1}(E) + 3x[J_1(E) - xJ] , \qquad B_1 = -\tfrac{1}{2}[J_1(E) - xJ] , \qquad B_s = J_1(E) - (1/2x)[J_1(E) + xJ] . \tag{4.7b}$$

Having derived expressions for the configurational averages of the irreducible components of the transformed Green's function, i.e., having determined $\langle \bar{g}_T \rangle^{T=0}$, we now have to give some thought to the problem of interpreting the significance of these expressions and to transforming them into an appropriate form suitable for numerical computation.

First, let us address ourselves to the fact that if we were to require a complete equality between the configurationally averaged Green's-function matrix, i.e., $\langle \bar{g}_T \rangle^{T=0}$, and the effective-medium Green's-function matrix $\bar{g}_T^{\text{eff}}$, then we would have the following three relations to satisfy self-consistently for all energies E:

$$\langle g_\eta \rangle^{T=0} = g_\eta^{\text{eff}} , \quad \eta \equiv p, d \tag{4.8}$$

$$\langle \bar{g}_s \rangle^{T=0} = \bar{g}_s^{\text{eff}} . \tag{4.9}$$

If this could be done, then we would have carried the (presently generalized) path CPA philosophy to consummation. Unfortunately, we notice very readily that while Eqs. (4.8) constitute two, linearly independent, scalar relationships, Eq. (4.9) is a matrix relationship involving another three matrix elements.

This state of affairs elicits at least two reactions.

One is, quite obviously, that we made an error in our basic formulation because we should have somehow introduced five self-consistent (complex) potentials, rather than only three effective-medium exchange integrals. The second reaction is that because we formulated our problem in terms of an effective medium involving a set of coherent-exchange integrals—the set was seen rather naturally to have only three members, $J_\mu(E)$, $\mu \equiv 1, 2, 3$—we should carry this analysis through by sticking to this philosophy.

In the present work, we have limited ourselves only to the latter of the two reactions. The more general formulation remains of interest and, at least at the time of this writing, we have plans to explore its possibilities. As is, however, clear, the present work is self-contained in its philosophy relating to isotropic coherent exchange integrals acting within a bilinear Heisenberg exchange model. And because its extension to the five-variable scheme seems necessarily to entail a change in the bilinear interspin exchange-integral format, we feel reassured about our present formulation.

In light of the above remarks, our next task is to evolve a single self-consistent condition from Eq. (4.9). This is done quite naturally by requiring the identity of the traces of the two matrices given in Eq. (4.9), i.e.,

$$\mathrm{Tr}\langle \bar{g}_s\rangle^{T=0} = \mathrm{Tr}\bar{g}_s^{\mathrm{eff}} . \tag{4.10}$$

The three conditions defining our CPA, i.e., Eqs. (4.8) and (4.10), in their present form, i.e., that contained in Eqs. (3.22) and (4.3) for Eq. (4.10) and Eqs. (3.23) and (4.1) for Eq. (4.8), are rather formal. In order to do computations we have to recast them in appropriate, explicit form. Such recasting is straightforward but tedious. Such recasting is straightforward but tedious. Therefore, for brevity, in the following we record only the most useful of the intermediate states in this process. First, let us deal with Eq. (4.10). We get

$$\bar{g}_s^{\mathrm{eff}} = \begin{vmatrix} \tau_0 & \sqrt{6}\tau_1 \\ \sqrt{6}\tau_1 & \tau_s \end{vmatrix} , \tag{4.11a}$$

where

$$\begin{aligned} \tau_0 &= \frac{1}{N}\sum_{\vec{K}} \tau_{\vec{K}}(E), \\ \tau_1 &= \frac{1}{N}\sum_{\vec{K}} \gamma_{\vec{K}}\tau_{\vec{K}}(E), \\ \tau_s &= \frac{1}{N}\sum_{\vec{K}} 6(\gamma_{\vec{K}})^2\tau_{\vec{K}}(E), \\ \tau_{\vec{K}}(E) &= [E - \Sigma_{\vec{K}}(E)]^{-1}, \\ \Sigma_{\vec{K}}(E) &= 6J_1(E)\gamma_{\vec{K}}(\gamma_{\vec{K}} - 1) + 3Z_p(E)(1 - \gamma_{2\vec{K}}) \\ &\quad + 3Z_d(E)[1 + \gamma_{2\vec{K}} - 2(\gamma_{\vec{K}})^2] . \end{aligned} \tag{4.11b}$$

Also,

$$\langle \bar{g}_s\rangle^{T=0} = x\begin{vmatrix} A_1 & A_2 \\ A_2 & A_3 \end{vmatrix} + (1-x)\begin{vmatrix} 0 & 0 \\ 0 & A_4 \end{vmatrix} , \tag{4.12a}$$

where

$$\begin{aligned} A_1 &= B_{00} + \tau_s/\tau_R , \\ A_2 &= \sqrt{6}\,(B_1 - \tau_1/\tau_R) , \\ A_3 &= B_s + \tau_0/\tau_R , \\ A_4 &= \tau_R[J_1(E)\tau_R + \tau_0]^{-1}, \quad \tau_R = \tau_0\tau_s - 6(\tau_1)^2 . \end{aligned} \tag{4.12b}$$

Unlike Eq. (4.10), Eq. (4.8) is quite simple, i.e.,

$$g_p^{\mathrm{eff}} \equiv \tau_p = \frac{1}{N}\sum_{\vec{K}} (1 - \gamma_{2\vec{K}})\tau_{\vec{K}}(E) \tag{4.13}$$

and

$$g_d^{\mathrm{eff}} \equiv \tau_d = \frac{1}{N}\sum_{\vec{K}} \frac{3}{2}[1 + \gamma_{2\vec{K}} - 2(\gamma_{\vec{K}})^2]\tau_{\vec{K}}(E) . \tag{4.14}$$

Using these simplified expressions for g_η^{eff}, we readily find those for $\langle g_\eta\rangle^{T=0}$ [i.e., by combining them with Eq. (4.1)].

Utilizing Eqs. (4.11a)–(4.14), we finally arrive at the following three relationships involving the stated unknowns $J_1(E)$, $Z_p(E)$, and $Z_d(E)$ of our theory:

$$\begin{aligned} Z_\eta(E) &= \tfrac{1}{2}[J_1(E) + xJ] \\ &\quad - \{Z_\eta(E) - (1/2x)[J_1(E) + xJ]\}\tau_\eta Z_\eta(E), \quad \eta \equiv p,\ d \end{aligned} \tag{4.15}$$

$$\begin{aligned} \tau_0 + \tau_s &= [x/Q(E)][\tau_0 + \tau_s + (B_s + B_{00})\tau_R] \\ &\quad + (1-x)\tau_R[\tau_0 + \tau_R J_1(E)]^{-1}, \end{aligned} \tag{4.16a}$$

where

$$\begin{aligned} Q(E) &= 1 + 12B_1\tau_1 + B_{00}\tau_0 + B_s\tau_s \\ &\quad + \tau_R(B_{00}B_s - 6B_1^2) . \end{aligned} \tag{4.16b}$$

[Note that B_{00}, B_1, B_s are the same as defined earlier in Eq. (4.7b).]

Having thus achieved an explicit statement of the self-consistent conditions, our next task is to specify what to do with them.

From the relationships (4.12a)–(4.14), we are able to determine the trace of the matrix $\bar{g}^{\mathrm{eff}}$, i.e.,

$$\begin{aligned} \mathrm{Tr}\bar{g}^{\mathrm{eff}} &= \mathrm{Tr}\langle \bar{g}\rangle^{T=0} \\ &= \langle g_{i,i}\rangle^{T=0} + \sum_\alpha \langle g_{\alpha,\alpha}\rangle^{T=0} = 7\tau_0 . \end{aligned} \tag{4.17}$$

By generalizing the usual single-site CPA philosophy, the effective medium determined in the present work is thus seen to lead to τ_0 as the Green's function of basic significance. Recalling the presence of the factor S^{eff} in the denominator in the definition of our Green's functions [see Eqs. (2.9)–(2.19)], it is convenient to introduce the notation

$$\Gamma^{(0)}(E) = S^{\mathrm{eff}}\tau_0 = x\tau_0 \tag{4.18}$$

and

$$\Gamma(\vec{K},E)=S^{\text{eff}}\tau_{\vec{K}}(E)=x\tau_{\vec{K}}(E) \quad . \tag{4.19}$$

The magnetic response function $\rho_{\vec{K}}(\omega)$ is thus given by the expression

$$\rho_{\vec{K}}(\omega) \underset{\epsilon\to+0}{=} -\frac{1}{\pi}\,\mathrm{Im}\Gamma(\vec{K},\omega+i\epsilon) \quad , \tag{4.20a}$$

and the density of states by the relation

$$\rho(\omega)=\frac{1}{N}\sum_{\vec{K}}\rho_{\vec{K}}(\omega)$$

$$\underset{\epsilon\to+0}{=} -\frac{1}{\pi}\,\mathrm{Im}\Gamma^{(0)}(\omega+i\epsilon) \quad . \tag{4.20b}$$

For arbitrary value of the magnetic concentration x, the solution of the coupled equations (4.15)–(4.16b) is nontrivial and can only be carried out numerically. For small impurity concentration, i.e., when $1-x \ll x$, analytical calculations, in various orders of the small parameter $1-x$, may be possible. In particular, to the first order in $1-x$ the calculations are straightforward and we present them below.

It is clear that when $x=1$, i.e., there are no empty sites, the system reduces to the case of a nonrandom, uniform Heisenberg ferromagnet with isotropic nearest-neighbor exchange J. Thus, in the limit $x=1$, the effective medium is identical to the pure system and we have

$$J_1(E)=Z_p(E)=Z_d(E)=J \quad ,$$

$$J_2(E)=J_3(E)=0 \quad .$$

Near this limit we look for Taylor-expansion type of solutions for $J_\mu(E)$, $\mu\equiv 1,2,3$. Equivalently, for $1-x \ll 1$ we write

$$\begin{aligned} J_1(E)&=J+\Delta_1(E)+O(1-x)^2 \quad , \\ Z_\eta(E)&=J+\Delta_\eta(E)+O(1-x)^2 \quad , \quad \eta\equiv p,d \end{aligned} \tag{4.21}$$

where we expect Δ_1 and Δ_η to be of the order $1-x$.

It is convenient to introduce the notation

$$F_\lambda=\lim_{x=1}(\tau_\lambda), \quad \lambda\equiv 0,1,s,p,d \tag{4.22}$$

[compare Eqs. (4.11b), (4.13), and (4.14) for the definition of τ_λ] such that F_λ are the effective-medium Green's functions for the pure ferromagnet, i.e.,

$$\begin{aligned} F_0&=\frac{1}{N}\sum_{\vec{K}}[E-6J(1-\gamma_{\vec{K}})]^{-1} \quad , \\ F_d&=\frac{1}{N}\sum_{\vec{K}}\frac{\frac{3}{2}[1+\gamma_{2\vec{K}}-2(\gamma_{\vec{K}})^2]}{E-6J(1-\gamma_{\vec{K}})} \quad , \end{aligned} \tag{4.23}$$

etc.

The foregoing statements refer to the pure case, i.e., $x=1$. This, therefore, constitutes the zeroth-order result.

To find the first-order result, we first iterate Eq. (4.15) to the next stage by using Eq. (4.21). We find

$$\Delta_\eta(E)=\tfrac{1}{2}[\Delta_1(E)+(1-x)J]+T_\eta(E), \quad \eta\equiv p,d \tag{4.24}$$

where

$$T_\eta(E)=-(1-x)J[1+JF_\eta]^{-1}, \quad \eta\equiv p,d \quad . \tag{4.25}$$

The T's defined above are recognized as being the corresponding p,d components of the T matrix referring to the impurity potential of an isolated, i.e., a single, vacancy.[8]

To determine $\Delta_1(E)$ we have to deal with Eqs. (4.16a) and (4.16b). Introducing the expressions given in Eq. (4.21) into Eq. (4.7b), we first evaluate B_χ, $\chi\equiv 00,1,s$:

$$B_{00}=-(1-x)(E-6J)+3[\Delta_1(E)+(1-x)J]+O(1-x)^2, \tag{4.26}$$

$$\begin{aligned} B_1&=-\tfrac{1}{2}[\Delta_1(E)+(1-x)J]+O(1-x)^2 \quad , \\ B_s&=\tfrac{1}{2}[\Delta_1(E)-(1-x)J]+O(1-x)^2 \quad . \end{aligned} \tag{4.27}$$

Because B_χ, $\chi\equiv 00,1,s$, is dominantly of order $1-x$ we can write Eq. (4.16a) as

$$[Q(E)-x][F_0+F_s]=\frac{F_1}{J}\left(-(B_{00}+B_s)+\frac{(1-x)}{F_1-F_0}\right). \tag{4.28}$$

Here we have utilized the following relationship among the pure-case Green's functions for a simple-cubic lattice:

$$F_0F_s-6F_1^2=-F_1/J \quad . \tag{4.29}$$

Next, we deal with Eq. (4.16b). Using Eq. (4.27) we get

$$Q(E)-x=(1-x)+12B_1F_1+B_{00}F_0+B_sF_s+O(1-x)^2 \quad . \tag{4.30}$$

After some algebraic manipulations, Eqs. (4.27), (4.28), and (4.29) yield the following result for $\Delta_1(E)$:

$$\Delta_1(E)=12J^2(1-x)F_0/[1-EF_0] + (1-x)J+O(1-x)^2 \quad . \tag{4.31}$$

Now combining Eqs. (4.11b) with Eqs. (4.21), (4.24), and (4.31) we find that in the limit of small vacancy dilution

$$[\tau_{\vec{K}}(E)]^{-1}=E-E_{\vec{K}}(1)-\{T^s_{\vec{K}}+3T_p^{(E)}(1-\gamma_{2\vec{K}}) + 3T_d(E)[1+\gamma_{2\vec{K}}-2(\gamma_{\vec{K}})^2]\} \quad , \tag{4.32}$$

where

$$E_{\vec{K}}(1)=6J(1-\gamma_{\vec{K}}) \quad , \tag{4.33}$$

$$T^s_{\vec{K}}=(1-x)E_{\vec{K}}(1)\left(1+\frac{E_{\vec{K}}(1)F_0}{1-EF_0}\right) \quad , \tag{4.34}$$

and $T_p(E)$ and $T_d(E)$ are the same as in Eq. (4.25). [Compare Eq. (4.11b).]

In the literature, e.g., Izyumov,[8] exact results for $T_p(E)$ and $T_d(E)$ are available. Our results, given in Eqs. (4.25) and (4.32), agree with these, giving us some confidence in our three-parameter path CPA schematization. Next, it is interesting to examine the s-symmetry component of the T matrix, i.e., $T^s_{\vec{K}}$, given in Eq. (4.34). In the literature, this quantity has been obtained by at least three different authors. The earliest result known to us was obtained by Izyumov,[8] who found it to be equal to $T^{s\,(I)}_{\vec{K}}$, where

$$T^{s\,(I)}_{\vec{K}} = (1-x)[E_{\vec{K}}(1)]^2/[E(1-EF_0)] \ . \qquad (4.35)$$

At resonance, i.e., $E = E_{\vec{K}}(1)$, this is clearly equal to our result [see Eq. (4.34)]. On the other hand, Elliott and Pepper, as quoted in Harris *et al.*,[1] are supposed to have found instead the expression $T^{s\,(EP)}_{\vec{K}}$, where

$$T^{s\,(EP)}_{\vec{K}} = (1-x)\left(\frac{F_0[E_{\vec{K}}(1)]^2}{1-EF_0} + 2E_{\vec{K}}(1) - E + \frac{[E-E_{\vec{K}}(1)]^2}{E-\Delta}\right), \qquad (4.36)$$

while Harris *et al.*[1] found the result $T^{s\,(HLNE)}_{\vec{K}}$,

$$T^{s\,(HLNE)}_{\vec{K}} = \frac{(1-x)E_{\vec{K}}(1)[E_{\vec{K}}(1)-6\Delta]}{(1-EF_0)(E-6\Delta)} \ , \qquad (4.37)$$

where in expressions (4.36) and (4.37) the quantity Δ is the strength of the pseudopotential introduced to take account of the spurious spin-wave degrees of freedom associated with the empty sites in these formulations. We see readily that upon resonance, the Elliott-Pepper result agrees with ours, while the Harris *et al.*[1] result does this in the limit $\Delta \to \infty$ (i.e., the limit in which the spurious degrees of freedom mentioned above should be completely suppressed).

Another interesting detail that emerges from the above analytical calculations is the behavior of the low-frequency, long-wavelength response in the limit of low vacancy concentration. The generally accepted result, correct to the order $1-x$, for the response is that it is like that of an undamped spin wave, ie, when $|\vec{K}| \to 0$, with energy stiffness $D_0(x)$ such that

$$D_0(x)/D_0(1) = [\Sigma_{\vec{K}}(E \approx \Sigma_{\vec{K}})/E_{\vec{K}}(1)]_{|\vec{K}|\to 0} = 1 - (1-x)\Lambda_{sc} - O(1-x)^2 \ , \qquad (4.38a)$$

where

$$\Lambda_{sc} \cong 1.532 \ . \qquad (4.38b)$$

Our computation for the parameter Λ_{sc} proceeds as follows: Because

$$\frac{D_0(x)}{D_0(1)} = \lim_{\substack{|\vec{K}|\to 0 \\ E\to\Sigma_{\vec{K}}(0)}} \frac{\Sigma_{\vec{K}}(E)}{E_{\vec{K}}(1)} = \lim_{E\to 0} \frac{2Z_p(E) - J_1(E)}{J} \ , \qquad (4.39)$$

hence

$$\Lambda_{sc} = (2/J)\,T_p(E \approx 0) - 1 \simeq 1.5316 \ . \qquad (4.40)$$

Here we used Eq. (4.25) and the fact that F_p at $E=0$ is $\cong -(1.5164 - 0.2571)/6J$, i.e.,

$$\left(\frac{1}{6J}\right)\frac{1}{N}\sum_{\vec{k}}\left(\frac{\gamma_{2\vec{K}}-1}{1-\gamma_{\vec{K}}}\right) = (F_p)_{E=0} \ .$$

It is satisfying to be able to reproduce the known results in the small-vacancy-concentration limit.

V. FREQUENCY MOMENTS

An accepted lore of the self-consistent effective-medium theories is that the number of exactly preserved frequency moments provides a useful gauge of their accuracy. On the other hand, the exact preservation of only a few of the frequency moments cannot *per se* be considered to be of any great intrinsic value since one knows that even when two given functions have an identical finite number of frequency moments, they can, in principle, differ arbitrarily from each other.[15]

Yet, because self-consistent theories are constructed to represent the dynamics of the actual random systems through the choice of appropriate effective media, one traditionally expects them to reproduce several of the lowest-order frequency moments exactly. Exact preservation of the higher-order moments is, however, often not achieved, in practice, for the notorious misrepresentation of the band-tailing effect[16] by effective-medium theories also concomitantly causes the higher-order frequency moments to be seriously underestimated. In the same vein, we might add that if any of the effective-medium theories are found to be exact to any given order in some appropriately chosen small parameter, e.g., $1-x$ in the present scheme, and also $1/z$ if one is working with arbitrary coordination[3] number z, then *all* the frequency moments are reproduced exactly to the appropriate order in terms of the relevant small parameter. For instance, because our theory has been seen to be reliable in the small impurity concentration limit, we can expect it to reliably reproduce frequency moments to the order $1-x$.

Let us define the νth, K-dependent frequency moment of the response function as

$$m^{(\nu)}_{\vec{K}} = \int_{-\infty}^{+\infty} \rho_{\vec{K}}(\omega)\,\omega^\nu\,d\omega \ . \qquad (5.1)$$

[See Eq. (4.20a) for the definition of $\rho_{\vec{K}}(\omega)$.] Because,

$$\Gamma(\vec{K},E) = S^{eff}\tau_{\vec{K}}(E) = \int_{-\infty}^{+\infty} d\omega\,\frac{\rho_{\vec{K}}(\omega)}{(E-\omega)} \ , \quad \mathrm{Im}E > 0 \qquad (5.2)$$

therefore,

$$\Gamma(\vec{K},E)=\sum_{\nu=0}^{\infty}\frac{m_{\vec{K}}^{(\nu)}}{(E)^{\nu+1}}\ . \tag{5.3}$$

The procedure for calculating the exact moments for the diluted ferromagnet was described in detail in a previous paper by one of us,[3] and the first few terms of the expansion for the exact Green's function have been given in Eq. (3.20) in Harris *et al.*'s paper,[1] i.e.,

$$\begin{aligned}
&(m_{\vec{K}}^{(0)})_{\text{exact}}=x\ ,\\
&(m_{\vec{K}}^{(1)})_{\text{exact}}=x^2E_{\vec{K}}(1)\ ,\\
&(m_{\vec{K}}^{(2)})_{\text{exact}}=x\{2(1-x)xJE_{\vec{K}}(1)+[xE_{\vec{K}}(1)]^2\}\ ,\\
&(m_{\vec{K}}^{(3)})_{\text{exact}}=x\{2(1-x)x(2+3x)J^2E_{\vec{K}}(1)\\
&\qquad+4(1-x)x^2JE_{\vec{K}}^2(1)+[xE_{\vec{K}}(1)]^3\},
\end{aligned} \tag{5.4}$$

where $E_{\vec{K}}(1)$ is the same as defined in Eq. (4.33) and x is the concentration of the magnetic atoms.

A formal expansion of $\tau_{\vec{K}}(E)$ is obtained from Eq. (4.11b) as follows:

$$\tau_{\vec{K}}(E)=\sum_{\nu=0}^{\infty}\frac{[\Sigma_{\vec{K}}(E)]^{\nu}}{E^{\nu+1}}\ , \tag{5.5}$$

where $\Sigma_{\vec{K}}(E)$ is itself given by the high-energy expansion

$$\Sigma_{\vec{K}}(E)=\sum_{n=0}^{\infty}\frac{L_{\vec{K}}^{(n)}}{E^n}\ , \tag{5.6}$$

$$\begin{aligned}
L_{\vec{k}}^{(n)}&=6J_1^{(n)}\gamma_{\vec{K}}(\gamma_{\vec{K}}-1)+3Z_p^{(n)}(1-\gamma_{2\vec{K}})\\
&\quad+3Z_d^{(n)}(1+\gamma_{2\vec{K}}-2\gamma_{\frac{2}{K}}^{2})\ ,
\end{aligned} \tag{5.7}$$

and where $J_1^{(n)}$, $Z_\eta^{(n)}$, $\eta\equiv p,\ d$, are the coefficients of E^{-n} in a high-energy expansion of $J_1(E)$ and $Z_\eta(E)$, $\eta\equiv p,d$.

By introducing Eq. (5.6) into Eq. (5.5) and remembering the S^{eff} occurring in Eq. (5.2) we get

$$\begin{aligned}
&m_{\vec{K}}^{(0)}=x\ ,\\
&m_{\vec{K}}^{(1)}=L_{\vec{K}}^{(0)}x\ ,\\
&m_{\vec{K}}^{(2)}=(L_{\vec{K}}^{(0)})^2x+xL_{\vec{K}}^{(1)}\ ,\\
&m_{\vec{K}}^{(3)}=(L_{\vec{K}}^{(0)})^3x+2xL_{\vec{K}}^{(0)}L_{\vec{K}}^{(1)}+xL_{\vec{K}}^{(2)}\ .
\end{aligned} \tag{5.8}$$

The values of the first few moments are obtained by introducing the expansion of Eq. (5.3) into Eqs. (4.11b), (4.13), (4.14), etc., and by expanding in a high-energy series the self-consistent equations (4.15)–(4.16b). The resulting algebra is extremely tedious. Finally we obtain

$$m_{\vec{K}}^{(\nu)}=(m_{\vec{K}}^{\nu})_{\text{exact}}\quad\text{for } \nu=0,\ 1,\ 2,$$

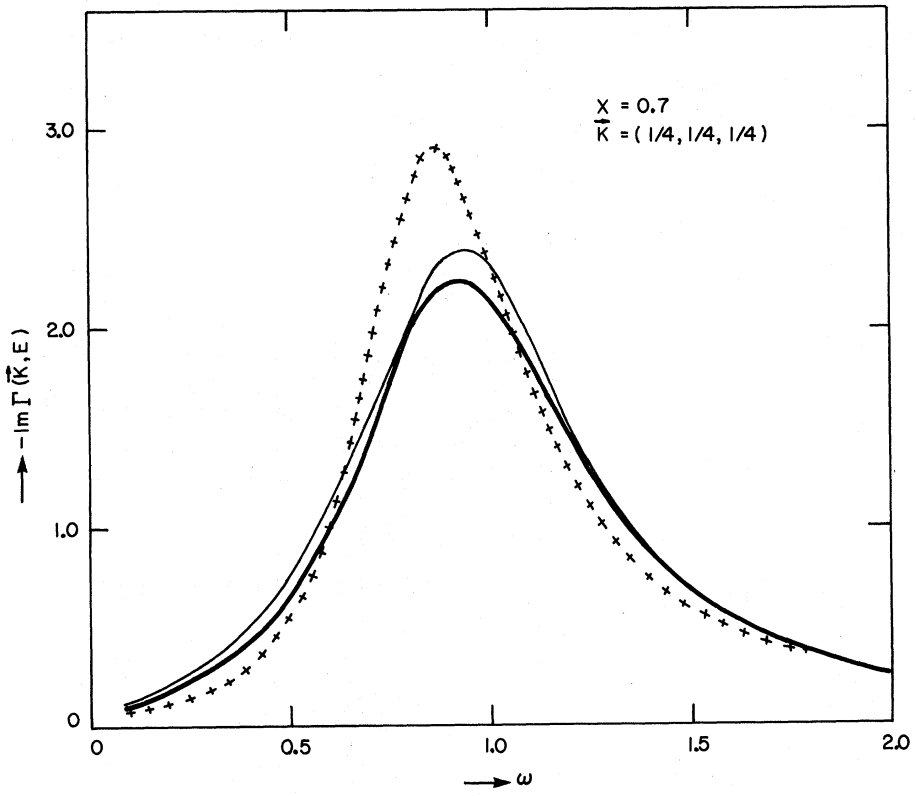

FIG. 2. Response, i.e., $-\mathrm{Im}\Gamma(\vec{K},E)$ for $E=\omega+0.06\,i$, is plotted as a function of ω for magnetic concentration $x=0.7$. $\vec{K}$ is along (k,k,k) direction and the given results are for $k=\frac{1}{4}\pi$. The *heavy* continuous line shows the Padé-moment procedure, i.e., the so called "exact," results while the *light* continuous line gives the results obtained by Harris *et al.* (Ref. 1). Our results are shown as crosses.

$$m_{\vec{K}}^{(3)} = x\{[xE_{\vec{K}}(1)]^3 + 4x^2(1-x)J[E_{\vec{K}}(1)]^2 + 2x(1-x)[2x+3]J^2E_{\vec{K}}(1)\}. \quad (5.9)$$

Upon comparing Eqs. (5.4) and (5.9), we find that our theory exactly preserves the first three moments of the spectral density while the fourth moment, i.e.,

$$m_{\vec{K}}^{(3)} = (m_{\vec{K}}^{(3)})_{\text{exact}} + 2x^2(1-x)^2J^2E_{\vec{K}}(1), \quad (5.10)$$

is in error by a term proportional to $(1-x)^2$. As mentioned earlier, the preservation of even-higher-order frequency moments to this order of accuracy can be reliably anticipated.

Finally, for the sake of completeness, let us add a word or two by way of explanation of the significance of the first few moments.

Clearly the conservation of $m_{\vec{K}}^{(0)}$ implies that the weight of the total magnetic response is being taken into account correctly. [Quite naturally, therefore, it is equal to the magnetic concentration x.] $m_{\vec{K}}^{(1)}$, on the other hand, refers to the center of gravity, i.e., the mean location of the maximum of the response. Moreover, it implies that in the limit $E \to \infty$, the effective-medium parameters are the same as given in a virtual-crystal type of an approximation, i.e.,

$$J_1(E) \underset{E\to\infty}{=} xJ,$$

$$J_\mu(E) \underset{E\to\infty}{\to} 0, \quad \mu = 2, 3. \quad (5.11)$$

This result therefore is expected in any moderately reasonable mean-field approximation. Thus the first nontrivial frequency moment which frequency-independent mean-field theories, e.g., the virtual-crystal approximation, do not preserve is $m_{\vec{K}}^{(2)}$. Also, because this is still a low-order moment, it is not too sensitive to the details of the band-tailing phenomenona.[15] Thus, it is encouraging to find its exact preservation, especially since the best and the most reliable CPA theory to date,[1] given by Harris *et al.*, does not conserve this moment for their best value of the pseudopotential, i.e., for $\Delta = \infty$.

VI. RESULTS

We shall conclude this paper by presenting in this section the various results of the numerical computations referred to in Sec. IV. Because the results for the low-impurity-concentration limit, i.e., $1-x \ll 1$, have already been described, we shall begin by describing the results in the intermediate-concentration regime.

A. Response at intermediate dilution: $x=0.7$

Harris *et al.* have supplied a set of spectral weight functions, i.e., the imaginary part of $\Gamma(\vec{K}, E)$ calculated at $E = \omega + i\,0.06$, in units such

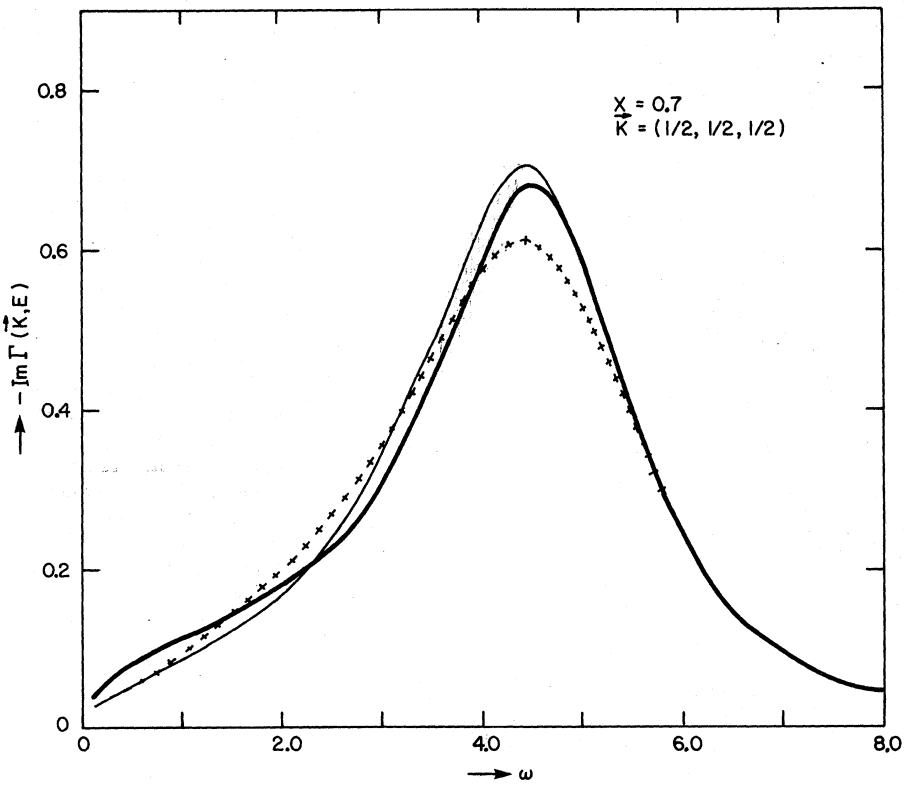

FIG. 3. Same as in Fig. 2 except that here $k = \frac{1}{2}\pi$.

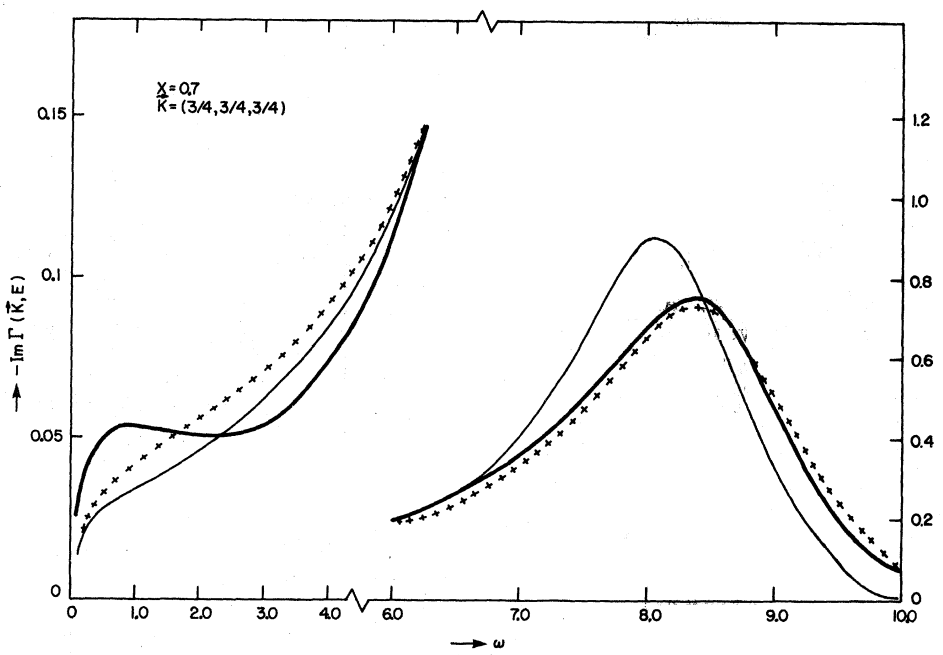

FIG. 4. Same as in Fig. 2 except here $k=\frac{3}{4}\pi$.

that the exchange constant is equal to 1 or, in other words, when the total bandwidth for the pure ferromagnet is 12. Clearly, in the limit that 0.06 can be considered to be vanishingly small compared with 12, these spectral weight functions are simply the frequency-wave-dependent magnetic-response functions, i.e., they are equal to $\pi\rho_{\vec{K}}(\omega)$, which embody all the needed information regarding the magnetic excitations in the system.

In Figs. 2–7 we have plotted $-\mathrm{Im}\Gamma(\vec{K}, E)$ for $E=\omega+0.06i$, or what we shall henceforth refer to as the *response*, for $x=0.7$, against ω for several values of $\vec{K}$. In these figures we present, in addition to our own results—which are plotted as crosses—the corresponding response calculated by Harris *et al.*[1]—as a continuous solid line—and the "exact" results generated by the Padé procedure based on the first ten numerically computed, exact frequency moments by Nickel[12]—drawn as the *heavy* continuous line.

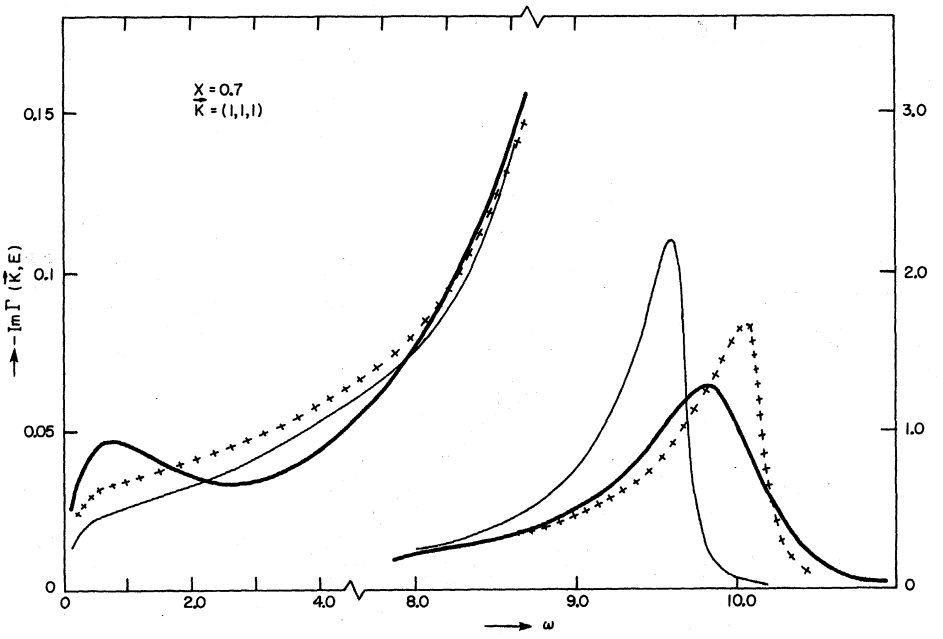

FIG. 5. Same as in Fig. 2 but for $k=\pi$.

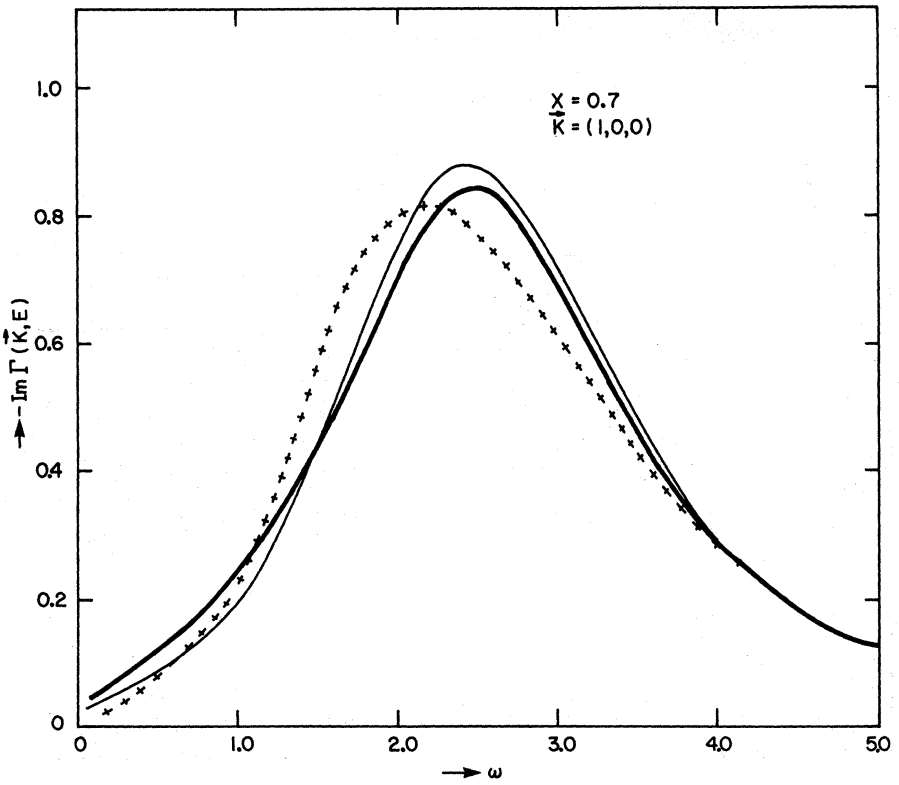

FIG. 6. Response for magnetic concentration $x = 0.7$ for $\vec{K} = (\pi, 0, 0)$. The curves are identified in the same way as in Fig. 2.

Looking along the (k, k, k) diagonal we see that for $k = \frac{1}{4}\pi$, our results are distinctly worse than those of Harris *et al.* (i.e., as compared with the exact-moment-procedure results), whereas halfway along the diagonal, i.e., $k = \frac{1}{2}\pi$, the mean-square deviation between our results and the exact[12] results (henceforth to be referred to as our MSD) is only about twice as large as the Harris *et al.* MSD. However, the situation is now shifting in our favor. Indeed, at $k = \frac{3}{4}\pi$ our results are over-

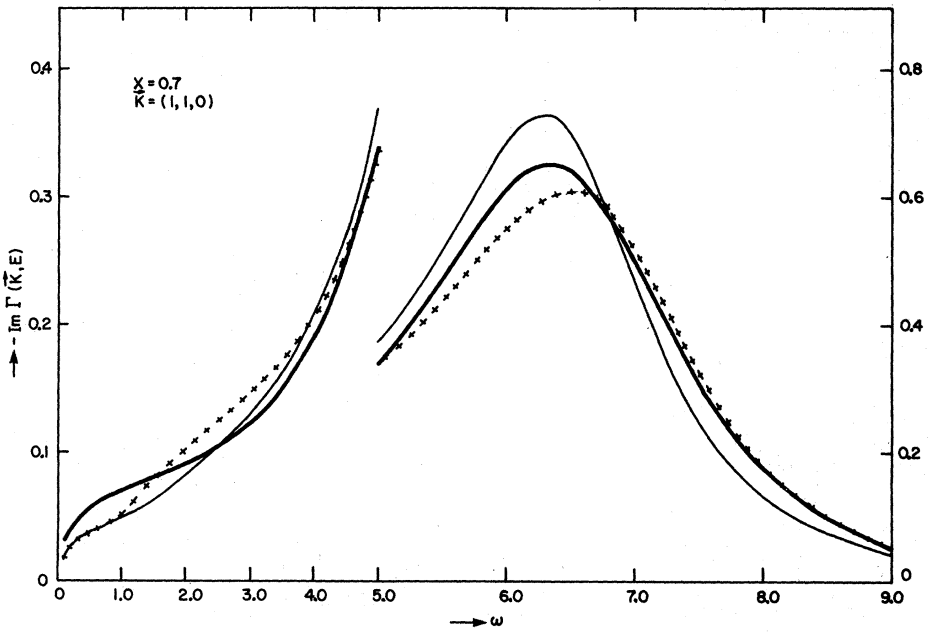

FIG. 7. Response for $x = 0.7$ for $\vec{K} = (\pi, \pi, 0)$. Curves are identified as in Fig. 2.

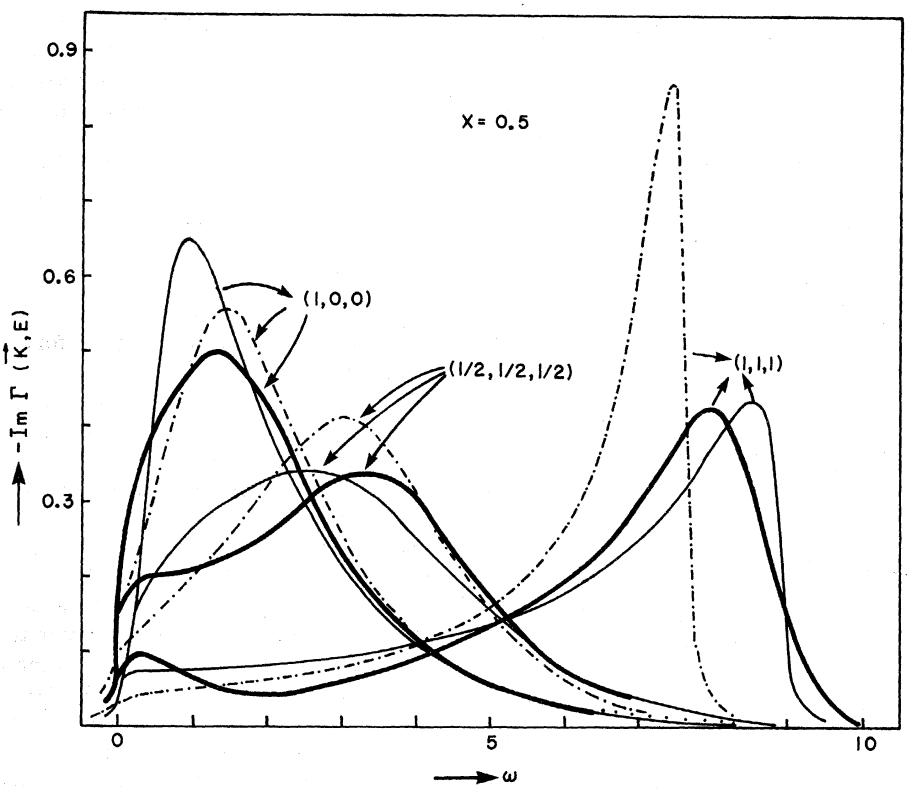

FIG. 8. Response for various $\vec{K}$ values for magnetic concentration $x = 0.5$. The three curves on the extreme right are for $\vec{K} = (\pi, \pi, \pi)$, while the middle three curves refer to $\vec{K} = (\frac{1}{2}\pi, \frac{1}{2}\pi, \frac{1}{2}\pi)$. The curves at the left-hand corner are for $\vec{K} = (\pi, 0, 0)$. Here the *heavy* curves are the exact, Padé-moment-procedure (Ref. 12) results; the continuous light curve gives *our* results while the dash-dot curve gives the results of Ref. 1.

whelmingly superior. (See Fig. 4.) Even at the diagonal zone edge, i.e., $k = \pi$, our MSD is only about a fifth of that of Harris *et al.* (See Fig. 5.)

Thus along the diagonal our score over all is better than (or, more conservatively, about the same as) that of Harris *et al.*'s theory. This we consider to be no mean feat, because the theory presented in Ref. 1 is the best CPA work to date applied to the sited-diluted ferromagnet.

Looking in other symmetry directions we find about the same situation. At $(\pi, 0, 0)$, i.e., Fig. 6, the Harris *et al.* MSD is about a half or so of that of ours while the opposite is true at $(\pi, \pi, 0)$, i.e., in Fig. 7.

B. Response at $x = 0.5$

When the vacancy concentration reaches the level of 50% of the total, the response is seriously damped. Although the moment calculations[12] do not converge as rapidly for $x = 0.5$ as they do for $x = 0.7$, they are still very reliable, as evidenced by their close correspondence with another exact numerical procedure used by Harris.[17]

In Fig. 8 we have plotted the response for various values of $\vec{K}$ for $x = 0.5$. Here our results are given as the light unbroken curve while Harris *et al.*'s results are presented as broken curves; the exact-moment-procedure results are again plotted as *heavy* continuous lines.

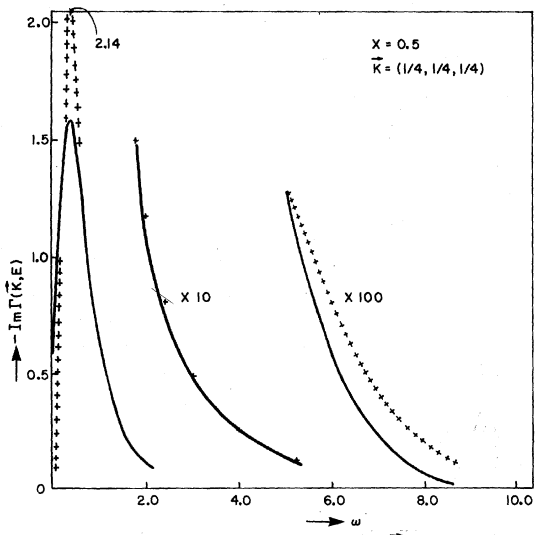

FIG. 9. Response for $x = 0.5$ along $\vec{K} = (k, k, k)$ for $k = \frac{1}{4}\pi$. The heavy continuous line refers to the moment-generated exact results (Ref. 12) while the crosses (given wherever the two sets of results differ) indicate our results. The scale factor (along the ordinate) is unity for the curve on the left, 10 for the middle curve, and 100 for the right-hand curve.

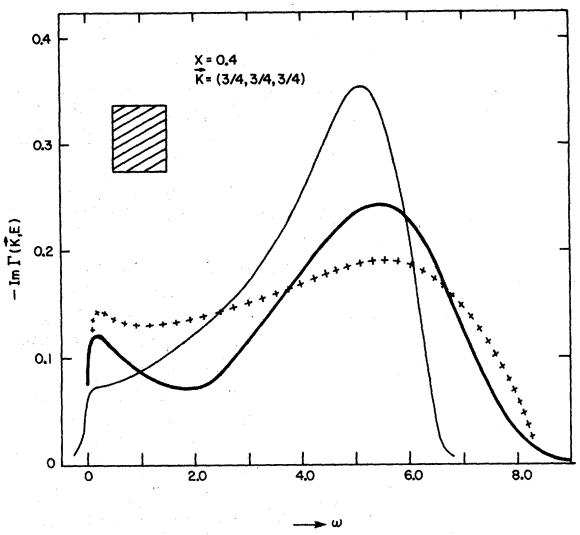

FIG. 10. Response along $\vec{K}=(k,k,k)$ for $k=\frac{3}{4}\pi$. The magnetic concentration here is 0.4. The curves are identified in the same way as in Fig. 2. The cross-hatched area indicates the weight of the *heavy* curve at $\omega \sim 0$. (See Ref. 12 for its description.)

We notice that near the zone edge, i.e., $\vec{K}=(\pi, \pi, \pi)$, our results closely resemble the exact ones (except for a small shift in the peak to a higher frequency). Indeed our MSD here is more than an order of magnitude smaller than that yielded by Harris *et al.*'s theory. Moreover, their response[11] visibly leaks into the negative-energy region. (Note that because the response is being measured slightly off the real axis, some leakage is to be expected, but its magnitude should be such that on the plotted scale it should be barely visible.)

Looking at the group of curves for $\vec{K}=(\frac{1}{2}\pi, \frac{1}{2}\pi, \frac{1}{2}\pi)$ and $\vec{K}=(\pi, 0, 0)$ we find that both the present theory and the Harris *et al.* CPA perform about evenly over most of the frequency scale, except at $\omega=0$, where our theory behaves somewhat better. (See Fig. 8.)

To test our results against the exact ones for their high-frequency detail, we have chosen a figure given in Ref. 12 (i.e., its Fig. 4 with its $\alpha=1$). In our Fig. 9, the response at $\vec{K}=\frac{1}{4}\pi(1,1,1)$ is plotted for $x=0.5$. For clarity, the scale is increased by a factor of 10 for intermediate frequencies and a factor of 100 for large frequencies. We find that except for a minor difference, i.e., the heights of the responses which occur in a very narrow range around the maximum, the two sets of results (ours are given as crosses whenever they do not fall on the exact results) are in surprisingly good agreement. Only at large frequency is the departure between the results visible. (Note that our results do terminate before the exact ones even though we do not record them for $\omega>9$. This is in accordance with the ubiquitously observed poor representation of band tailing effects by effective-medium theories.) A source of some satisfaction to us is the fact that this set of results, i.e., Fig. 9, is for "small" values of $\vec{K}$

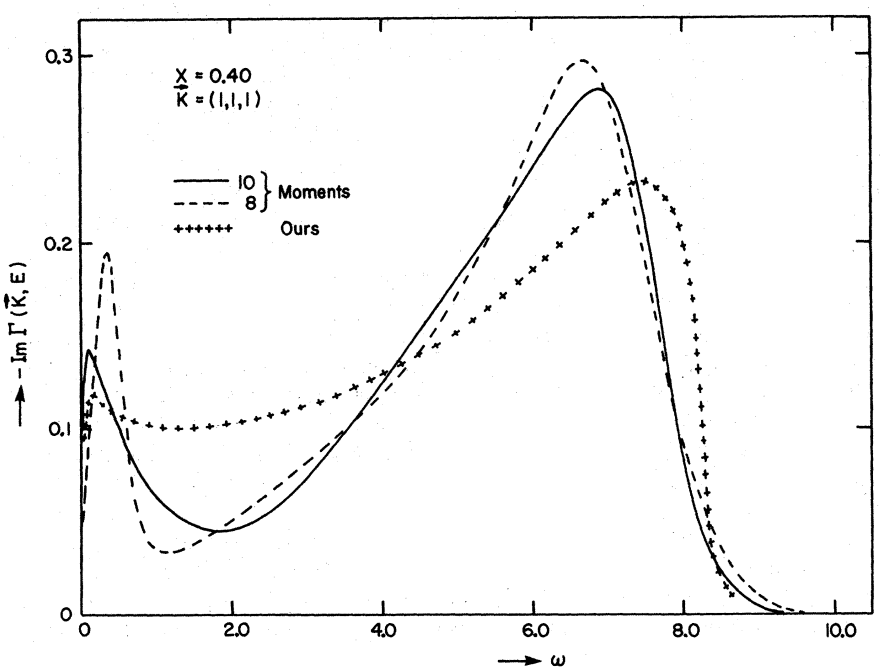

FIG. 11. Response at $\vec{K}=(\pi,\pi,\pi)$ for $x=0.4$. The continuous solid curve gives the Padé-moment-procedure results for the (5,5) Padé while the dashed curve gives the corresponding exact results using the (4,4) Padé. Our results are shown as crosses.

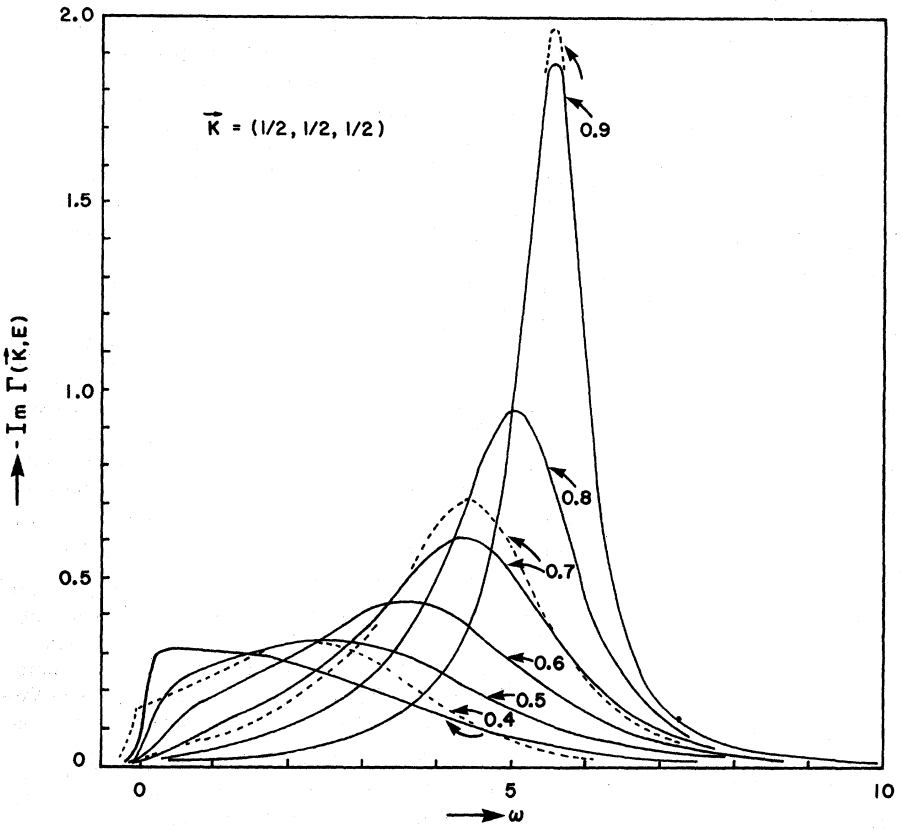

FIG. 12. Response for $\vec{K}=(\frac{1}{2}\pi, \frac{1}{2}\pi, \frac{1}{2}\pi)$. The full lines indicate the present results whereas the dashed lines indicate the corresponding results obtained in Ref. 1. Note that for $x=0.9$, the two set of results are indistinguishable from each other except at the top of the peak, where the Harris *et al.* results indicate a higher and a somewhat narrower peak. For $x=0.4$, we note the appreciable leakage of the Harris *et al.* (dashed curve) response into the negative region. For $x=0.8$, 0.6, and 0.5, we have only plotted our own results because the corresponding results of Ref. 1 were not readily available.

along the (k, k, k) diagonal. Traditionally, the present theory does less well for k less than about half the zone edge, while it does generally better for larger k values. (Compare, for example, Figs. 2–5 and 8.)

C. Response at $x=0.4$

Let us look next at the large-vacancy-concentration case, $x=0.4$. Here in Fig. 10, for $k=\frac{3}{4}\pi$, we have plotted our results (as crosses) along with those given by Harris *et al.*'s theory (a thin line) and the Padé-moment procedure[12] (*heavy* line). Again the MSD for our results is lower than that of Harris *et al.* At the diagonal edge, i.e., $\vec{K}=(\pi, \pi, \pi)$, we have plotted in Fig. 11 our results, as crosses, and those following from the Padé-moment procedure.[12] To demonstrate the measure of reliability of the exact results in this large-impurity-concentration range, we have given the results obtained from the (4, 4) Padé—dashed curve—and the (5, 5) Padé—solid curve. Clearly, the spread between the (5, 5) results and those given by our theory (shown as crosses) is somewhat larger than that between the same and the (4, 4) Padé results. Yet, these results help confirm our view that the present work constitutes a reasonable attempt at constructing an effective-medium theory which remains qualitatively useful even in the large-concentration limit.

D. General concentration

To get a feeling for how the response varies as a function of dilution, we look next at Fig. 12, where the response is plotted as a function of the frequency for $\vec{K}=(\frac{1}{2}\pi, \frac{1}{2}\pi, \frac{1}{2}\pi)$. For magnetic concentrations 0.9, 0.7, and 0.4, we also include the corresponding results obtained by Harris *et al.* (given as dotted lines wherever they differ from our results). We note that our theory generally predicts a broader response. Also the width increases with the increase of dilution.

In Fig. 13 (top section) we show the position of the main response peak, i.e., $E_{\vec{K}}(x)$, relative to its position in the nonrandom perfect system, i.e., $E_{\vec{K}}(1)$, for $\vec{K}$ along the diagonal (k, k, k), as a function of k. The upper most curve shows the results for magnetic concentration $x=0.9$, the middle curve refers to $x=0.7$, while the lowest curve (in the top section of Fig. 13) refers to $x=0.4$. Our results are plotted as crosses.

For small impurity concentration, i.e., $x=0.9$, our results are indistinguishable from those obtained in Ref. 1 (hence we have plotted no crosses there), while for larger vacancy concentration there are departures. For $x=0.7$, i.e., the in-

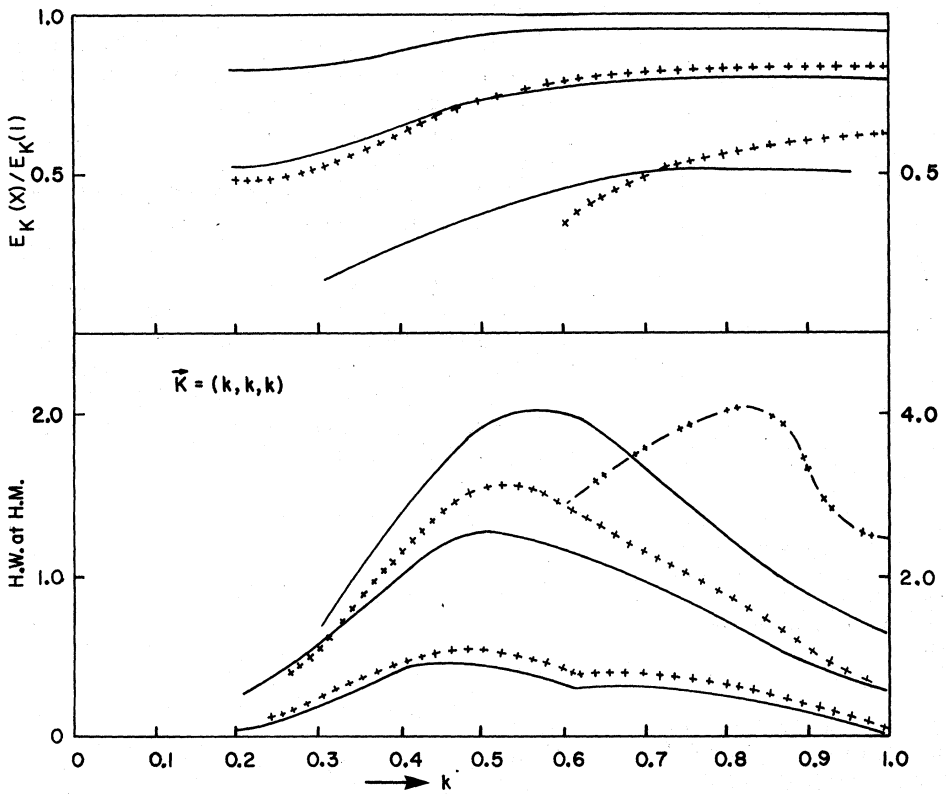

FIG. 13. Top section shows the results for the ratio of the positions of the main response peak for various magnetic concentrations x i.e., $E_{\vec{K}}(x)$, to that in the pure system, i.e., $E_{\vec{K}}(1)$, for $\vec{K} = \pi(k,k,k)$ as a function of k. The top curve refers to $x=0.9$, the middle one to $x=0.7$, and the bottom one to $x=0.4$. The continuous lines refer to the results of Ref. 1. Our results for $x=0.9$ are indistinguishable from those given in Ref. 1. For $x=0.7$ our results are not recorded for $k < 0.6$ for the reason explained in the text. Again the crosses indicate our results for $k>0.6$. The lower section of this figure gives the results for the half-width of these peaks (determined at half of the maximum height). The lowest curve refers to the case $x=0.9$ while the middle curves refer to $x=0.7$. For $x=0.4$ only the results of Ref. 1 (continuous lines) are given for all k. Our results are recorded for $k>0.6$. (For $x=0.4$ our result is indicated as a curve with dashes and crosses).

termediate-vacancy-concentration case, our $E_{\vec{K}}(x)$ lies somewhat lower than that obtained in the work of Harris *et al.* for $k<\frac{1}{2}\pi$. Around the middle of the zone, i.e., $k\sim\frac{1}{2}\pi$, the results coincide, while for $k>\frac{1}{2}\pi$ our results lie higher.

The behavior of our theory for the large-impurity case, i.e., $x=0.4$, is quite different from that of Ref. 1 for $k<0.6\pi$ or so. Here, our results in general show two peaks. The one at the low-frequency end tends to dominate in height for smaller k values. However, its location is a slowly varying function of k. As such, we have not plotted our results for these k values. For $k\gtrsim 0.6\pi$, the high-frequency peak (in our results for the response) begins to dominate quite distinctly and we can therefore plot these results in the given context. The location of the peak, i.e., $E_{\vec{K}}(x)$, is however somewhat smaller than that given by Harris *et al.* for $k\lesssim 0.72\pi$, while the reverse is true for $k\gtrsim 0.72\pi$. Thus for large vacancy concentrations our results have begun to differ, rather substantially, from those of Ref. 1.

In the bottom section of Fig. 13 we have plotted half-width of the corresponding peaks in the response. (This half-width is measured in units of J and is taken at half-maximum value of the response.) For $x=0.9$ (lowest curves) our results (given as crosses) mirror closely those given by Harris *et al.* except for the fact that our widths are somewhat larger. For $x=0.7$, (the middle curves) the behavior of the two sets of results is similar but the relative increase in the widths, over those given in Ref. 1, has become larger. On the other hand, for the large-vacancy case the structure of our results has become visibly different (see the top curves). Our results for $x=0.4$ are plotted as a curve with crosses and long dashes. For $k\gtrsim 0.55\pi$, the Harris *et al.* results show a monotonic decrease as k increases while our results attain a maximum for $k\sim 0.83\pi$.

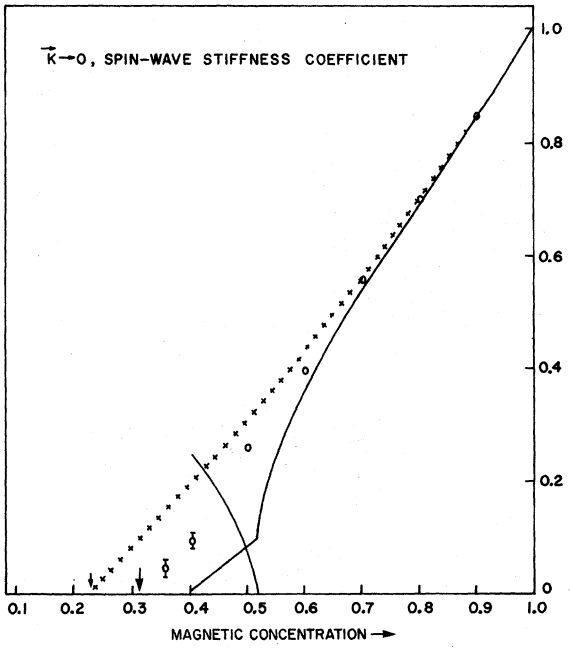

FIG. 14. Long-wavelength, i.e., $|\vec{K}| \to 0$, spin-wave stiffness is given as a function of the magnetic concentration. The continuous dark line gives the results of Ref. 1. Our results, wherever they differ, are given as crosses. The percolation-theory Monte Carlo results of Ref. 5 are indicated as circles.

Next, in Fig. 14, we plot the magnitude of the long-wavelength, spin-wave stiffness coefficient $D_0(x)/D_0(1)$ as a function of the magnetic concentration. Our results are given as crosses, the results of Ref. 1 as continuous lines, while the percolation-theory–Monte Carlo results[5] are given as circles. We find that our results closely agree with the other two for small, i.e., $\lesssim 0.2$, concentrations of the vacancies. For $0.5 < x \lesssim 0.8$, our results are in fair agreement with the percolation-theory–Monte Carlo results. Note that below about $x < 0.52$ the Harris *et al.* results break down completely. When the impurity concentration is as large as 60%, i.e., $x = 0.4$, our result for $D_0(x)/D_0(1)$ is almost twice that given by the percolation–Monte Carlo procedure. We feel that this, i.e., 60%, specifies the largest impurity concentration for which our theory is giving qualitatively useful results.

The sum of the response over the entire Brillouin zone—which would give the total density of states $\pi\rho(\omega)$ if we had used the limit $\epsilon \to 0$ in $E = \omega + i\epsilon$ [see Eq. (4.20b)] but which is only approximately equal to $\pi\rho(\omega)$ because we are using the approximation $\epsilon = 0.06$—i.e., $-\mathrm{Im}\Gamma^{(0)}(\omega + 0.06i)$, is plotted in Fig. 15. The top half of the figure gives the results obtained in the present paper. For small impurity concentration, e.g., $x = 0.9$, the density of states shows minor oscillations at the small-frequency end. These oscillations arise entirely due to the approximations involved in our numerical computations and they get damped down for larger randomness, i.e., when x is reduced, and the curves became smooth. We notice that the weight of the curves generally shifts towards the smaller-frequency region as the impurity concentration is increased. (Compare also Ref. 3.) In the bottom half of the figure, for the sake of comparison we give our results (as continuous lines) along with the Harris *et al.* results (as broken lines, whenever they differ from our results). For $x = 0.9$ our results are almost identical with Harris *et al.* [the fact that their results do not contain the undulations (referred to above) in the small-frequency region is completely immaterial because they are an artifact of our approximate computational procedure]. For $x = 0.7$ differences between our results and those given in Ref. 1 are beginning to be apparent. Our results show a tendency toward putting greater weight towards

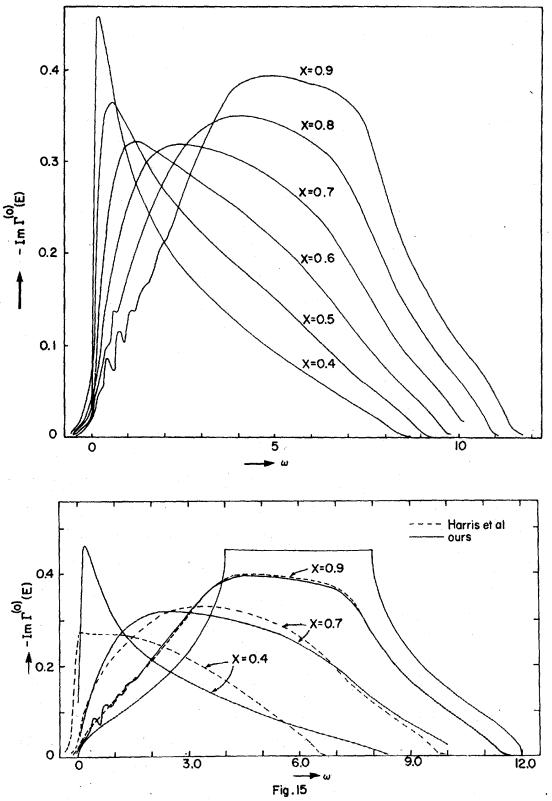

FIG. 15. Density of states, i.e., $-\mathrm{Im}\Gamma^{(0)}(E)$ for $E = \omega + 0.06i$, is given for various magnetic concentrations x. The top section refers to our results only. In the bottom section our results are given as solid lines, while the Harris *et al.* results are indicated as broken lines (wherever they differ visibly from ours). For low concentration, e.g., $x = 0.9$, the undulations near the low-frequency end are a result of the approximate computational procedure used here.

a lower-frequency region. For large vacancy concentration, i.e., $x=0.4$, the differences between the two sets of results have become quite substantial. In particular, here the Ref. 1 density of states have visibly leaked into the disallowed (negative frequency) region.

Finally, in Figs. 16–18 we display the behavior of $J_1(E)$, $J_2(E)$, and the complex effective stiffness coefficient $D(E)$, where

$$D(E)=J_1(E)+4\left[J_2(E)+J_3(E)\right], \tag{6.1}$$

$$\lim_{|\vec{K}|\to 0}\frac{\Sigma_{\vec{K}}(E)}{6J(1-\gamma_{\vec{K}})}=D(E), \tag{6.2}$$

as a function of the frequency ω. We note that $J_1(E)$ completely dominates the other two coherent exchange integrals, except in the very-large-impurity-concentration region, where the "effective" number of magnetic nearest neighbors becomes small.

E. Remarks

We conclude this paper by noting briefly that here we have presented an alternative procedure for achieving a CPA-like approximation for describing excitations in a randomly diluted Heisenberg ferromagnet. The accuracy of the results of this procedure is fully comparable to that of Ref. 1, in the small- and intermediate-vacancy-concentration regimes. For large vacancy concentration, i.e., $0.6\gtrsim x\gtrsim 0.4$, our results seem to be of superior quality to those given in Ref. 1 (which is the best CPA work to date). Also, in terms of low-order frequency-moment preservation, the present work gives a better performance than Ref. 1.

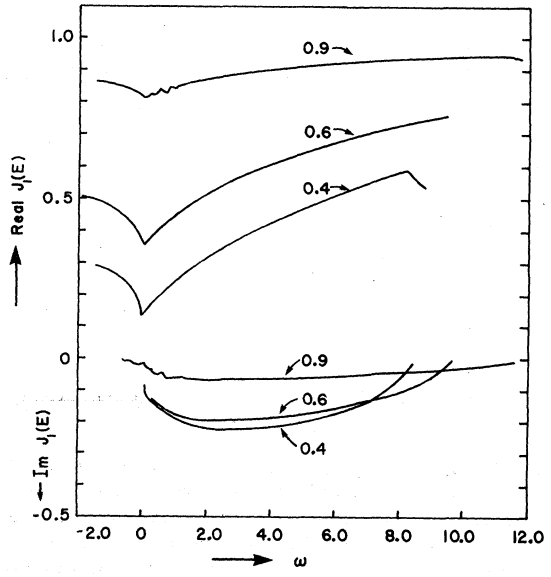

FIG. 16. Real and imaginary parts of the nearest-neighbor effective-medium exchange integral $J_1(E)$ for $E=\omega+0.06i$. The magnetic concentrations are indicated on the curves.

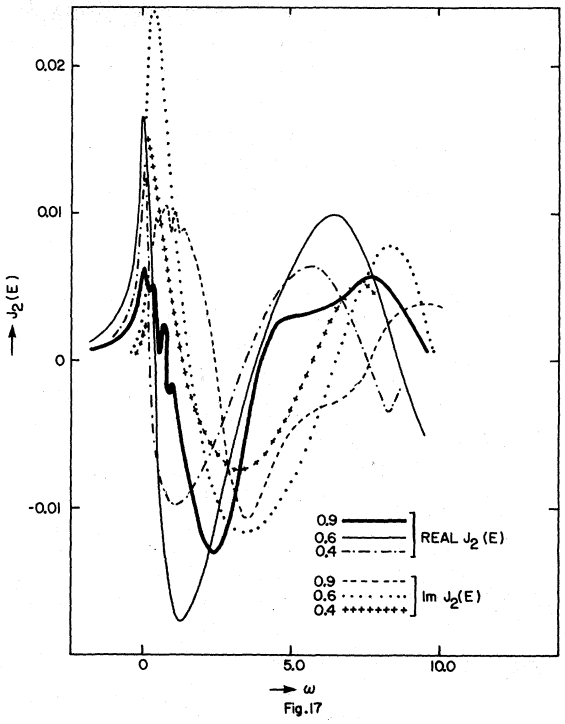

FIG. 17. Same as in Fig. 15 except these results are for $J_2(E)$ and moreover for the sake of clarity the various curves are identified in the right lower corner of the figure.

ACKNOWLEDGMENTS

Initial impetus for this work was provided by our discussions with Dr. François Brouers, to whom we

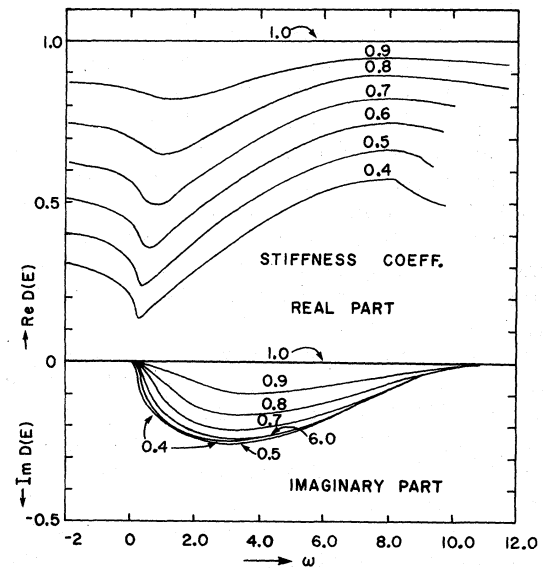

FIG. 18. Here we give the effective stiffness coefficient $D(E)=J_1(E)+4[J_2(E)+J_3(E)]$ for $E=\omega+0.06i$.

express our gratitude. We are grately indebted to Professor R. J. Elliott for his hospitality during a six weeks stay in Oxford. We benefitted greatly from discussions with him and with Dr. William Holcomb. We are also indebted to Professor Brooks Harris for a helpful discussion concerning Ref. 1. Lastly, we express our gratitude to the Computer Centers at Oxford University and Temple University for the use of their facilities, and to the National Science Foundation for enabling A. T. to work for a time at Temple University and to the NATO-NSF authorities for the granting of a Senior Fellowship to R. T-K. for visiting Oxford University.

---

*Present address: Facultad de Ciencias Exactas y Naturales, Departmento de Fisica, Ciudad Universitaria, Núnez, Buenos Aires, Argentina.

†Supported by NSF Grant No. GH39023.

[1]A. Brooks Harris, P. L. Leath, B. G. Nickel, and R. J. Eliott, J. Phys. C 7, 1693 (1974).

[2]A. Theumann, J. Phys. C 6, 2822 (1973); 7, 2328 (1974).

[3]R. A. Tahir-Kheli, Phys. Rev. B 6, 2808 (1972).

[4]R. C. Jones, J. Phys. C 4, 2903 (1973).

[5]S. Kirkpatrick, Phys. Rev. Lett. 27, 1722 (1971); Solid State Commun. 12, 1279 (1973); S. Kirkpatrick and V. K. S. Shante, Adv. Phys. 20, 325 (1971).

[6]D. Kumar and A. Brooks Harris, Phys. Rev. B 8, 2166 (1973).

[7]T. Wolfram and J. Callaway, Phys. Rev. 130, 2207 (1963).

[8]Yu. Izyumov, Proc. Phys. Soc. Lond. 87, 505 (1966).

[9]P. Soven, Phys. Rev. 156, 809 (1967); D. W. Taylor, Phys. Rev. 156, 1017 (1967).

[10]R. J. Elliott and D. E. Pepper, Phys. Rev. B 8, 2374 (1973).

[11]T. Matsubara, Prog. Theor. Phys. Suppl. 53, 202 (1973).

[12]B. G. Nickel, J. Phys. C 8, 1719 (1974).

[13]R. A. Tahir-Kheli and D. ter Haar, Phys. Rev. 127, 88 (1962).

[14]F. Brouers, F. Ducastelle, F. Gautier, and J. Van der Rest, J. Phys. F 3, 2120 (1973); F. Brouers, M. Cyrot, and F. Cyrot-Lackmann, Phys. Rev. B 7, 4370 (1973); F. Brouers and F. Ducastelle, J. Phys. F. (to be published).

[15]W. C. Grant, Physica 30, 1433 (1964).

[16]I. M. Lifshitz, Adv. Phys. 13, 483 (1964).

[17]A. Brooks Harris (unpublished work using Monte Carlo procedures for computing the response, private communication).